TKK Dissertations 105
Espoo 2008

DIFFERENT APPROACHES FOR SURFACE MODIFICATIONS: FORMATION OF INHIBITIVE FILM ON COPPER SURFACES AND SURFACES FUNCTIONALISED WITH Ag NANOPARTICLES

Doctoral Dissertation

Kirsi Yliniemi

Helsinki University of Technology
Faculty of Chemistry and Materials Sciences
Department of Chemistry

TKK Dissertations 105
Espoo 2008

DIFFERENT APPROACHES FOR SURFACE MODIFICATIONS: FORMATION OF INHIBITIVE FILM ON COPPER SURFACES AND SURFACES FUNCTIONALISED WITH Ag NANOPARTICLES

Doctoral Dissertation

Kirsi Yliniemi

Dissertation for the degree of Doctor of Science in Technology to be presented with due permission of the Faculty of Chemistry and Materials Sciences for public examination and debate in Auditorium Ke2 at Helsinki University of Technology (Espoo, Finland) on the 28th of March, 2008, at 12 noon.

Helsinki University of Technology
Faculty of Chemistry and Materials Sciences
Department of Chemistry

Teknillinen korkeakoulu
Kemian ja materiaalitieteiden tiedekunta
Kemian laitos

Distribution:
Helsinki University of Technology
Faculty of Chemistry and Materials Sciences
Laboratory of Physical Chemistry and Electrochemistry
P.O. Box 6100
FI - 02015 TKK
FINLAND
URL: http://www.tkk.fi/Units/PhysicalChemistry/
Tel. +358-9-451 2572
Fax +358-9-451 2580
E-mail: kirsi.yliniemi@tkk.fi

ISBN 978-951-22-9226-4
ISBN 978-951-22-9227-1 (PDF)
ISSN 1795-2239
ISSN 1795-4584 (PDF)
URL: http://lib.tkk.fi/Diss/2008/isbn9789512292271/

TKK-DISS-2429

Multiprint Oy
Espoo 2008

ABSTRACT OF DOCTORAL DISSERTATION	HELSINKI UNIVERSITY OF TECHNLOGY P.O. BOX 1000, FI-02015 TKK http://www.tkk.fi

Author Kirsi Yliniemi

Name of the dissertation
Different Approaches for Surface Modifications: Formation of Inhibitive Film on Copper Surfaces and Surfaces Functionalised with Ag Nanoparticles

Manuscript submitted 28th November 2007	Manuscript revised N/A
Date of the defence 28th March 2008	
☐ Monograph	☒ Article dissertation (summary + original articles)

Faculty	Faculty of Chemistry and Materials Sciences
Department	Department of Chemistry
Field of research	Electrochemistry
Opponent(s)	Prof. Patrik Schmuki
Supervisor	Prof. Kyösti Kontturi
(Instructor)	

Abstract

The purpose of this study was to investigate different surface modifications and two different approaches have been studied in this Thesis. In the first part, the purpose was to study the mechanism for the formation of inhibitive copper-benzotriazole [Cu(I)-BTA] film and in the second part, the surface modifications were done with Ag nanoparticles to create for example antibacterial surfaces. The formation of an inhibitive [Cu(I)-BTA] film on copper and copper alloy surfaces has been investigated as a function of potential, alloying element and oxygen content in the surrounding environment. Measurements were performed using scanning electrochemical microscope (SECM) with which the change from a conductive to an insulating surface can be detected. The potential of copper substrate was observed to have a crucial effect on the formation of inhibitive [Cu(I)-BTA] film. At positive potentials (from -0.2 V to open circuit potential) the formation of the film can be detected as a function of exposure time for benzotriazole (BTAH). At negative potentials the copper surface stayed conductive even after four hours exposure leading to a conclusion that no inhibitive film can form on the surface. This leads to a final conclusion that adsorption is not enough for the inhibition of copper. Also, the effect of alloying elements (in this study silver and phosphorus) was observed. Both of these elements decreased the rate of film formation and in the case of silver enrichment on the surface, film formation was totally absent. Moreover, the role of oxygen in the film formation was studied in this thesis and it was observed that oxygen is needed for the formation of inhibitive film on copper surface. In addition, surface modifications with Ag nanoparticles – which possess interesting properties like antibacteriality and Surface-Enhanced Raman Scattering (SERS) – have been studied. When Ag nanoparticles are embedded into the sol-gel films it was observed that their presence increased the barrier properties of the film. Furthermore, the stability of the films was able to be improved by low temperature O_2 and H_2 plasma treatments. A novel route for the formation of ultra-thin films with attached Ag nanoparticles is outlined in this Thesis. Ultra-thin films do not show antibacterial properties, inducing that attached nanoparticles are not antibacterial in the tested system but sufficient amount of dissolution of silver is needed. This study also questions the currently widely used testing methods. SERS activity of the ultra-thin films is not observed but with a slight modification in synthesis to create thicker films containing more Ag on the surface produces good SERS enhancement. The enhancement factor is $1 \cdot 10^7$ which is a relatively high value when thinking of practical applications as a SERS probe.

Keywords copper, benzotriazole, stainless steel, Ag nanoparticles, antibacteriality

ISBN (printed)	978-951-22-9226-4	ISSN (printed)	1795-2239
ISBN (pdf)	978-951-22-9227-1	ISSN (pdf)	1795-4584
Language	English	Number of pages	64+52 (app.)
Publisher	Department of Chemistry		
Print distribution	Laboratory of Physical Chemistry and Electrochemistry, P.O. Box 6100, 02015 TKK, Finland		

☒ The dissertation can be read at http://lib.tkk.fi/Diss/2008/isbn9789512292271/

VÄITÖSKIRJAN TIIVISTELMÄ	TEKNILLINEN KORKEAKOULU PL 1000, 02015 TKK http://www.tkk.fi
Tekijä Kirsi Yliniemi	
Väitöskirjan nimi Erilaisia lähestymistapoja pintojen muokkaukseen: suojaavan kerroksen muodostuminen kuparin pinnalle ja pintojen funktionalisointi Ag nanopartikkeleilla	
Käsikirjoituksen päivämäärä 28.11.2007	Korjatun käsikirjoituksen päivämäärä N/A
Väitöstilaisuuden ajankohta 28.3.2008	
☐ Monografia	☒ Yhdistelmäväitöskirja (yhteenveto + erillisartikkelit)
Tiedekunta Kemian ja materiaalitieteiden tiedekunta Laitos Kemian laitos Tutkimusala sähkökemia Vastaväittäjä(t) Prof. Patrik Schmuki Työn valvoja Prof. Kyösti Kontturi (Työn ohjaaja)	

Tiivistelmä

Tässä väitöskirjassa on tutkittu erilaisia lähestymistapoja pintojen muokkaukseen. Ensimmäisen osan tavoitteena on ollut selvittää suojaavan kupari-bentsotriatsolikerroksen [Cu(I)-BTA] muodostumismekanismia ja toisen osan tavoite on ollut tutkia pintojen muokkausta Ag nanopartikkeleilla lähinnä niiden antibakteeristen ominaisuuksien takia.Suojaavan [Cu(I)-BTA]-kerroksen muodostumista tutkittiin kuparin ja kupariseosten pinnalle potentiaalin, kupariseokseen lisättävän alkuaineen tai ympäristön happipitoisuuden funktiona. Pintoja tutkittiin sähkökemiallisella pyyhkäisymikroskoopilla (SECM), jonka avulla voidaan tutkia johtavan pinnan muuttumista eristäväksi pinnaksi. Kuparin potentiaali vaikuttaa suojaavan [Cu(I)-BTA]-kerroksen muodostumiseen. Positiivisilla potentiaaleilla (-0.2 V:sta avoimen virtapiirin potentiaaliin) kerroksen muodostuminen tapahtui bentsotriatsolin (BTAH) altistusajan funktiona; negatiivisilla potentiaaleilla suojaavaa kerrosta ei havaittu edes neljän tunnin altistusajan jälkeen eli suojaavaa kerrosta ei muodostu pinnalle. Tästä voidaan päätellä että pelkkä BTAH:n adsorptio ei ole riittävä suojaamaan kuparipintaa. Myös kupariseokseen lisättävät alkuaineet (fosfori ja hopea) hidastivat suojaavan kerroksen muodostumista. Hopea esti kokonaan kerroksen muodostumisen suurilla hopeapitoisuuksilla. Hapen läsnäolo todettiin välttämättömäksi suojaavan kerroksen muodostumisessa.Lisäksi tässä työssä tutkittiin pintojen muokkausta Ag nanopartikkeleilla, joilla on monia mielenkiintoisia ominaisuuksia kuten antibakteerisuus tai nk. SERS-aktiivisuus eli ne voivat vahvistaa Raman spektriä moninkertaisesti. Kun Ag nanopartikkelit muodostettiin sol-gel-kerroksen sisälle, ne estivät paremmin liuoksen tunkeutumista kerroksen läpi. O_2- ja H_2 –plasmakäsittelyillä sol-gel-kerrosten stabiilisuus kasvoi. Tässä työssä esitellään myös uusi tapa valmistaa hyvin ohuita Ag nanopartikkelikerroksia siten, että nanopartikkelit ovat tiukasti pinnassa kiinni. Nämä ohuet kerrokset eivät osoittaneet bakteerien kasvun hidastumista antibakteerisuuskokeissa eli tiukasti kiinnitetyt nanopartikkelit eivät itsessään ole antibakteerisia tutkitussa systeemissä, vaan hopean liukeneminen pinnalta on välttämätön. Lisäksi tässä työssä kyseenalaistetaan tällä hetkellä runsaasti käytettyjen testimenetelmien sopivuutta vastaavankaltaisiin tilanteisiin. Ohuiden kalvojen SERS-aktiivisuutta ei myöskään havaittu, mutta pienellä muutoksella synteesiprosessissa voitiin valmistaa paksumpia kalvoja, jotka sisältävät enemmän Ag nanopartikkeleita. Nämä kerrokset ovat SERS-aktiivisia ja niiden SERS-vahvistuskerroin on jopa $1 \cdot 10^7$, joka on riittävän korkea arvo ajatellen käytännön sovelluksia SERS-anturina.

Asiasanat kupari, bentsotriatsoli, ruostumaton teräs, Ag nanopartikkeli, antibakteerisuus			
ISBN (painettu)	978-951-22-9226-4	ISSN (painettu)	1795-2239
ISBN (pdf)	978-951-22-9227-1	ISSN (pdf)	1795-4584
Kieli	englanti	Sivumäärä	64+52 (liitteet)
Julkaisija	Kemian laitos		
Painetun väitöskirjan jakelu	Fysikaalisen kemian ja sähkökemian laboratorio, PL 6100, 02015 TKK, Finland		
☒ Luettavissa verkossa osoitteessa http://lib.tkk.fi/Diss/2008/isbn9789512292271/			

Preface

The work presented in this Thesis has been done during 2002-2007 in the Laboratory of Physical Chemistry and Electrochemistry at Helsinki University of Technology, in the group of Adhesion and Thin Films at Max-Planck Institute for Iron Research and in the Department of Metallurgy, Materials and Electrochemistry at Vrije Universiteit Brussel. I acknowledge TEKES (Finnish Funding Agency for Technology and Innovation), Fortum Foundation and Outokumpu Oyj Foundation for the financial support of this work.

I have learnt a lot – and not only about surface modifications – when working on this project. There are number of people who have helped me to realise this Thesis and I want to thank all of you for your contributions, however big or small. My greatest gratitude belongs to Prof. Kyösti Kontturi for supervising this Thesis. Without his optimistic and supporting comments this Thesis would have never been finished. Also, I want to thank Dr. Anna-Kaisa Kontturi, Dr. Christoffer Johans and Dr. Lasse Murtomäki for all the help during my time at FyKe.

Prof. Guido Grundmeier I thank for the warm invitation to Max-Planck Institute and for all the discussions, both scientific and personal ones, whenever we meet. Prof. Herman Terryn I acknowledge for his kind and generous offer to visit his laboratory at VUB, also understanding the need for co-operation not only between the labs but between people. In addition, I want to thank all of the co-authors for the brainstorming and interesting ideas in our papers, especially Lic.Sc.(Tech.) Marjatta Vahvaselkä for introducing me to the interesting world of antibacterial testing methods.

The whole FyKe group I thank for the maddest and craziest - in a positive way! - working atmosphere and special thanks belong to the following persons: Lic.Sc.(Tech.) Mari Aaltonen (without tea and discussions with you I could have never finished this, not even started!), Dr. Marja Vuorio, Ms. Marjukka Ikonen, Dr. Timo Laaksonen, Lic.Sc.(Tech) Päivi Ahonen, Dr. Ville Saarinen, Mr. Petri Kanninen and Mr. Thomas

Tingelöf, all of you I thank for helping me in many of life's hurdles (sometimes in unpractical ways, I agree).

Herr Dr. Stromberg, Farbror Henrik, Dr. Belen, 002 and Queen Kirsten I thank for making my time in the No1 City to be such a positive and important experience in my life. Without frequent visits to Altstadt with you I could have not been so active at work. The friends here in Finland I thank for the relaxing, sometimes rather absurd moments (like picnics in sun, rain and snow), which have been able to keep me going with this project; especially I want to mention Hapo, for understanding even when I thought it would have been impossible to understand and Eeva Eevuli, for stress-relieving late night discussions, both at work and outside work.

This Thesis would have never seen daylight without my parents and their endless love, without the home to where I can always come, both when it is sunny or when it is dark. My grandparents – also those who are no longer with us – I want to thank for all the encouragement during my whole life. Finally, my Fellow Communers I want to thank for those numerous, extremely therapeutic moments on our Red Sofa: my sister Sanna, for guiding me through my life and always believing in me during this time even if sometimes I did not believe myself and Ben - BroRap, for your constant support and making Parallel Universe to come true.

Kirsi Yliniemi

Espoo, 27th November 2007

Table of Contents

List of Publications ..... **i**

Author's contribution ..... **ii**

List of Abbreviations ..... **iii**

List of Symbols ..... **v**

List of Figures ..... **vii**

List of Tables ..... **viii**

1 Introduction **1**

2 Inhibition of Copper Corrosion with Benzotriazole **3**

2.1 Adsorption of BTAH and Formation of the Complex Film 4

2.2 Role of Oxygen in Formation of Inhibitive Film 6

2.3 Scanning Electrochemical Microscope (SECM) 9

2.3.1 Principles of Feedback Mode of SECM 10

2.4 Studies of Inhibition of Copper Corrosion with Benzotriazole (Publications I-III) 14

2.4.1 Effect of Potential and Alloying Element (Publications I and II) 14

2.4.2 Effect of Oxygen (Publication III) 19

2.5 Summary of Inhibition of Copper Corrosion Studies 20

3 Surface Modifications with Silver Nanoparticles **22**

3.1 Applications of Ag Nanoparticles 23

3.1.1 Antibacterial Properties of Silver 23

3.1.2 Raman Scattering and SERS Activity of Silver 25
3.1.3 Optical Switches 25
3.2 Background to Sol-Gel Films with Ag Nanoparticles 26
3.3 Studies of Silver Nanoparticle Containing Sol-Gel Films (Publication IV) .. 29
3.3.1 Effect of Plasma Treatments on Nanoparticles and Matrix 29
3.4 Background to Ultra-Thin Films 33
3.5 Studies of Ultra-Thin Films (Publication V) 35
3.5.1 Formation of the Ultra-Thin Films 35
3.5.2 SERS and Antibacterial Activity 40
3.6 Summary of Studies of Surface Modifications with Ag Nanoparticles 44

4 Conclusions 46

5 References 48

List of Publications

This thesis consists of an overview and of the following publications which are referred to in the text by their Roman numerals.

I. K. Mansikkamäki, P. Ahonen, G. Fabricius, L. Murtomäki, K. Kontturi, Inhibitive Effect of Benzotriazole on Copper Surfaces Studied by SECM, *J. Electrochem. Soc.* **152** (2005) B12-B16.

II. K. Mansikkamäki, U. Haapanen, C. Johans, K. Kontturi, M. Valden, Adsorption of Benzotriazole on the Surface of Copper Alloys Studied by SECM and XPS, *J. Electrochem. Soc.* **153** (2006) B311-B318.

III. K. Mansikkamäki, C. Johans, K. Kontturi, The Effect of Oxygen on the Inhibition of Copper Corrosion with Benzotriazole, *J. Electrochem. Soc.* **153** (2006) B22-B24.

IV. K. Yliniemi, P. Ebbinghaus, P. Keil, K. Kontturi, G. Grundmeier, Chemical composition and barrier properties of Ag nanoparticle-containing sol-gel films in oxidizing and reducing low-temperature plasmas, *Surf. Coat. Technol.* **201** (2007) 7865-7872.

V. K. Yliniemi, M. Vahvaselkä, Y. Van Ingelgem, K. Baert, B.P. Wilson, H. Terryn, K. Kontturi, The Formation and Characterisation of Ultra-Thin Films Containing Ag Nanoparticles, *J. Mater Chem.* **18** (2008) 199-206.

Author's contribution

In Publications I-III, Kirsi Yliniemi (previously Mansikkamäki) did all the SECM measurements as well as modelling and interpreting of the SECM results.

In Publication IV, the optimising of the synthetic route and the preparation of most of the samples as well as all UV/Vis measurements were performed by the author. She also had an active role in FT-IRRAS, Electrochemical Impedance measurements and in interpreting the results, with the exception, the plasma treatments of the samples, EIS modelling and the measuring and modelling ToF-SIMS and spectroscopic Ellipsometry results.

In Publication V, Yliniemi created the synthetic route used in the study, prepared all the samples and performed all UV/Vis measurements. The Field-Emission Auger electron spectroscopy measurements, SERS studies and antibacterial tests were done in collaboration with co-authors. Analysis of the results was predominantly carried out by the author.

In all publications, Yliniemi has been responsible for the writing of the papers.

Espoo, 27th November 2007

Prof. Kyösti Kontturi

List of Abbreviations

AFM	atomic force microscope
Ag/AgCl	silver/silver chloride reference electrode
BTAH	benzotriazole
CFU	Colony Forming Units
CuAg	silver copper alloy
[Cu(I)-BTA]	cuprous benzotriazole complex
CuO	copper(II) oxide
Cu_2O	copper(I) oxide
DHP	phosphorus-deoxidised copper
DIAMO	3-(2-aminoethylamino)propyl trimethoxysilane
EF	SERS enhancement factor
EIS	Electrochemical Impedance spectroscopy
EQCM	electrochemical quartz-crystal microbalance
fcc	face-centered-cubic
FcMeOH	ferrocene methanol
FE-AES	Field-Emission Auger Electron Microscope
FTIR	Fourier Transformed Infrared spectroscopy
FT-IRRAS	FTIR Reflection Absorption Spectroscopy
GLYMO	3-(glyxidoxypropyl)-trimethoxy silane
HCl	hydrochloric acid
LbL	Layer-by-Layer
MEMO	3-(methacryloxypropyl)-trimethoxy silane
OCP	open circuit potential
OF-HC	oxygen free–dehydrated copper
PMT	phenylmercaptotetrazole
ppm	parts per million
SAM	self-assembly monolayer
SEM	Scanning Electron Microscope

SHE	standard hydrogen electrode
SCE	standard calomel electrode
SECM	scanning electrochemical microscopy
SERS	surface-enhanced Raman scattering
smSERS	single molecule SERS
STM	scanning tunnelling microscope
TEOS	tetraethyl-orthosilicate
ToF-SIMS	Time of flight-secondary ion mass spectrometry
UME	ultramicroelectrode
UV/Vis	ultraviolet – visible light spectroscopy
XPS	X-ray photoelectron spectroscopy

List of Symbols

a	radius of the SECM tip
A(L)	area of laser hitting the surface
A_m	area of one molecule
c_i	concentration of species i
C_i	dimensionless concentration of i
c_i°	bulk concentration of species i
δ	thickness of the film
d	distance between the SECM tip and the substrate
D_i	diffusion coefficient of i
e	electron
E	potential
F	Faraday's constant
i	current
i_{lim}	limiting current
I	dimensionless current
I(bulk)	Intensity of pure material in Raman spectra
I(surf)	Intensity of a material on a studied surface in Raman spectra
j	current density
J	dimensionless current density
$k_{f/b}$	rate constant of forward (f) or backward (b) reaction
$K_{f/b}$	dimensionless rate constant of forward (f) or backward (b) reaction
Λ	variable equal to $K_{f,S}L$
L	dimensionless distance between the SECM tip and the substrate (d/a)
n	number of electrons, normal to the surface
N_A	Avogadro's number
O	oxidized species
r	radius, radial coordinate in cylindrical coordination

R	reduced species, dimensionless radial coordinate in cylindrical coordination (r/a), roughness of a surface
S	denotation of substrate (as a subscript)
t	time
T	dimensionless time, denotation of tip (as a subscript)
V(L)	volume of laser travelling through the solution to the surface
z	vertical coordinate in cylindrical coordination
Z	dimensionless vertical coordinate in cylindrical coordination (z/a)
$\chi^{(3)}$	third-order optical non-linear susceptibility

List of Figures

Figure 1. Schematic figure of the formation of Cu(I)-BTA film versus adsorption of BTAH on copper/copper oxide surface.

Figure 2. Schematic figure of the feedback mode of SECM.

Figure 3. Approach curves as a function of exposure time measured at different substrate (DHP copper) potentials.

Figure 4. Approach curves as a function of exposure time measured at different substrate (OF-HC) potentials.

Figure 5. Approach curves as a function of exposure time measured at different substrate (CuAg, Ag>2%wt) potentials.

Figure 6. Approach curves to OF-HC copper as a function of exposure time to BTAH measured at open circuit potential at different oxygen contents.

Figure 7. UV/Vis spectra of sol-gel films containing Ag nanoparticles as a function of exposure time in air and light with and without O_2 plasma treatment.

Figure 8. UV/Vis spectra of sol-gel films containing Ag nanoparticles as a function of exposure time in air and light with and without O_2 and H_2 plasma treatments.

Figure 9. Schematic model of the effect of plasma treatments on sol-gel films containing Ag nanoparticles.

Figure 10. a) UV/Vis spectra of ultra-thin films on glass substrate as a function of annealing time.

Figure 11. a) UV/Vis spectra of ultra-thin films on stainless steel substrate as a function of annealing time.

Figure 12. Schematic figure of the formation of ultra-thin films containing Ag nanoparticles using DIAMO as an anchoring molecule.

Figure 13. Raman spectra of PMT solution on different surfaces.

List of Tables

Table 1. The thickness values (δ) of [Cu(I)-BTA] film as a function of potential after 4h exposure for BTAH containing solution in a normal atmosphere.

1 Introduction

Surface modification –a broad concept as it is – can be roughly divided into two categories: the surface modifications are either done to improve (and protect) material and its properties or they are used to bring totally new functionalities to the material. In this Thesis examples of both types of surface modifications are studied and therefore, this Thesis can also be divided into two parts: 1) the formation of [Cu(I)-BTA] films on copper and copper alloy surfaces and 2) the functionalisation of stainless steel surfaces with silver nanoparticles. In the first section the surface modifications are done mainly for the protection of copper from corrosion whilst in the second case new functionalities such as Surface Enhanced Raman Scattering (SERS) and antibacterial activity brought about by Ag nanoparticles on surfaces are studied.

The field of corrosion inhibition with benzotriazole has been studied for decades but still the mechanism is not well understood[1, 2, 3, 4]. During the last decade new experimental tools have been developed and for example in the first part of this Thesis a new approach that answers these previously unsolved problems has been found by using scanning electrochemical microscope (SECM).

Nanoparticle modified surfaces, on the other hand, have become a popular research topic during the last decade due to many extraordinary properties of the nanoparticles[5]. For example, the antibacterial nature[6] and the surface-enhanced Raman scattering (SERS)[7] activity of silver nanoparticles have caused lots of debate. In particular, sol-gel films in which Ag nanoparticles are embedded have been studied extensively[8]; however, often the stability and barrier properties of films are not well understood. Especially the effects due to nanoparticles and the matrix cannot be easily distinguished. Furthermore, while research has mainly focused on the development of properties with surface modifications using nanoparticles, also unknown health risks of nanoparticles have begun to cause concern[9,10]. Therefore, there is a clear need also to develop nanoparticle modified surfaces in which the nanoparticles are tightly bonded onto the surface.

In this work the surface modification of metals have been studied from different points of view through the combination of electrochemical methods to those used commonly in surface science and it has resulted in a broader understanding of the mechanism of the formation of [Cu(I)-BTA] film on the surface. Furthermore, nanoparticle modified surfaces have been studied where the demand for tight attachment of nanoparticles on the surface has been taken into account.

2 Inhibition of Copper Corrosion with Benzotriazole

The first part of this Thesis consists of corrosion inhibition studies of copper alloys with benzotriazole (BTAH) and this chapter introduces both a background to the studies with scanning electrochemical microscope (SECM), including the formation of the inhibitive film and the theory of SECM, and the main results of the studies in Publications I-III.

Copper is a widely used material mainly due to its excellent thermal and electronic properties. Additionally, copper is known to be a very good corrosion resistant material, however, in some media corrosion takes place and inhibitors are needed.[1] The selection of the right inhibitor has become even more important recently due to the high performance demands in conductivity in the case of new electronic applications[11].

Benzotriazole (BTAH) is the most common inhibitor utilised in the copper industry and its use predominates in many different applications. The excellent inhibitive effect of BTAH has been known already for several decades and even though it is commonly accepted that the inhibitive effect is due to a polymeric [Cu(I)-BTA] film on the copper surface, the formation of the film is still widely discussed. For example, at open circuit potential [Cu(I)-BTA] multilayers are formed by Cu-N bonds[1, 12] but the role of oxygen in the formation of the [Cu(I)-BTA] film[2, 3, 13, 14, 15, 16, 17], the orientation and binding of the BTAH molecule [12,18,19,20] have not been solved in detail. In addition, the role of potential, concentration and pH in the competition between the adsorption process and the complex formation of BTAH on copper surface has been studied intensively [4,21, 22]. Furthermore, the wide variety of areas in which copper and copper alloys are used also makes the effect of alloying element important.

In this Thesis the formation of the inhibitive film has been studied as a function of potential and alloying elements. Also, the role of oxygen in the formation has been investigated. The copper alloys selected to be studied are oxygen free–dehydrated

copper (OF-HC, < 10 ppm oxygen), phosphorus-deoxidised copper (DHP) and CuAg alloy. OF-HC is used in applications, which demand high conductivity and therefore the amount of impurities in it is extremely low. However, in manufacturing of OF-HC, optimising the amount of the additives is extremely difficult and some of them may remain in the copper lattice leading to a reduction in copper conductance due to scattered electrons in the lattice. For instance, it has been found that phosphorus has a significant influence on conductance even at the ppm level in copper alloys. Therefore, DHP, which has a high strength but lower conductivity, is mostly used in piping and tubing rather than in electrical applications. In contrast, it has been found that for example silver has only a minor effect on conductivity even in higher concentrations and CuAg alloy (0.25 % Ag) has been developed for electrical applications which demand high strength even at elevated temperatures. [23, 24,]

2.1 Adsorption of BTAH and Formation of the Complex Film

Both the pH and potential affect the adsorption of BTAH molecules and complex formation of the [Cu(I)-BTA] film. The trend found in literature is that in negative potentials and in acidic environments the adsorption of BTAH molecules predominates while the alkaline solutions and more positive potentials favour the formation of the inhibitive complex film.[4, 21, 22, 25] This is illustrated in Figures 1a and 1b and it is discussed briefly in this section. Also, some propositions for the adsorption of BTAH molecule on clean, oxygen free surfaces are illustrated in Figure 1c and the role of oxygen is discussed in more detail in Section 2.2.

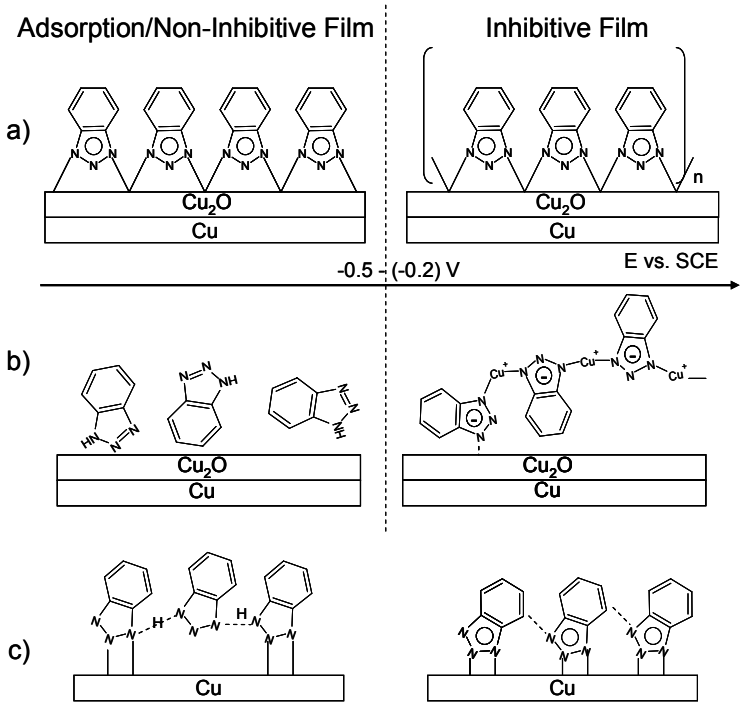

Figure 1. Schematic figure of the formation of [Cu(I)-BTA] film versus adsorption of BTAH on copper/copper oxide surface: a) the proposed dependence of the film structure on potential according to Gu and co-workers[4,25], b) the formation of the multilayer film from randomly adsorbed BTAH molecules in a solution according to Ling et al.[26], c) the proposed chemisorption of the first layer in the absence of oxygen according to Jiang and Adams[27] (left) and according to Fang et al.[17] (right).

For example, Youda *et al.*[21] proposed that there is equilibrium between the adsorption and the complex formation: in neutral solutions the film formation can take place in the whole potential range while in acidic solutions the adsorption of BTAH molecules dominates at negative potentials. Also Gu and co-workers[4] have observed the adsorption of BTAH molecule on the copper surface at negative potentials (from -0.7 to -0.3 V vs. Ag/AgCl) whilst at more positive potentials (up to 0.2 V vs. Ag/ AgCl) a polymeric film of $[Cu(I)\text{-}BTA]_n$ was formed in the acetonitrile solutions. According to Chan and Weaver[22], the adsorbed benzotriazole molecules deprotonate in an acidic media on the copper surface at potentials more positive than -0.3 – (-0.2) V vs. SCE and the further formation of [Cu(I)-BTA] film may take place.

The division according to potentials is not so clear. For example, another study of Gu and co-workers[25] shows that the composition of the film changes as a function of potential. They suggest that the polymeric complex film, $[Cu(I)\text{-}BTA]_n$, is converted to a $[Cu(I)\text{-}BTA]_4$ film at negative potentials between -0.5 and -1.1 V vs. SCE in neutral chloride solutions, because the lower potential results in lower pH and higher H^+ ion concentration at the electrode surface, which results in decomposition of the $[Cu(I)\text{-}BTA]_n$ to $[Cu(I)\text{-}BTA]_4$. Furthermore, according to Schultz *et al.* [28] BTAH adsorbs in a well ordered manner in its deprotonated form, BTA^-, instead of neutral BTAH on Cu(1 0 0) in the whole potential region (-0.65 – 0.20 V vs. Ag/AgCl), while on Cu(1 1 1) the layer is disordered at negative potentials and ordered at positive potentials.

Bastidas[29] and co-workers[30] have used gravimetric methods to study the adsorption of benzotriazole on copper surface by comparing different adsorption isotherms. They observed that Frumkin's isotherm described the behaviour of adsorption of BTAH on copper surface best in the set of the 11 isotherms. Yu *et al.*[13] have modelled the adsorption with Langmuir isotherm. However, these studies do not distinguish between the complex formation and adsorption but the surface coverage is calculated from the inhibition efficiency which is estimated either from the gravimetric results[29, 30] or from the Cu^{2+} ion solution analysis[13].

2.2 Role of Oxygen in Formation of Inhibitive Film

As stated earlier, the inhibitive effect of BTAH is due to the formation of polymeric complex on the copper surface [13]. However, the role of oxygen in the formation of the inhibitive film has not been solved fully and the main questions remain as to whether or not oxygen is needed for the adsorption of BTAH on the surface and whether or not oxygen – either in the form of atmospheric oxygen or in cuprous oxide - is needed for the formation of the inhibitive complex layer.

In general, two different opinions of the role of oxygen in the adsorption and film formation process have been suggested: some studies suggest that the adsorption of BTAH and even the film formation, for example by hydrogen bonds, is possible onto clean, oxygen free copper surfaces[17, 27, 31]. Other studies support the theory that the adsorption is possible onto clean surfaces but oxygen enhances it and the formation of inhibitive [Cu(I)-BTA] film is more pronounced when oxygen is present[16,26].

In addition, the difference between atmospheric oxygen (i.e. O_2) and oxygen bound in the metal oxide (i.e. Cu_2O) on the adsorption and the film formation mechanism has been studied[32]. The adsorption of BTAH on metallic copper in air was observed when the sample was etched before immersion into BTAH solution. The mechanism proposed was that first, Cu(0)-BTAH film forms and then [Cu(I)-BTA] film is formed through reaction with O_2 and copper as shown in Reaction 1[32]:

$$\mathrm{BTAH + Cu(0) \rightarrow Cu(0)BTA \xrightarrow{(Cu)-O_2(ads)} Cu^{+}BTA^{-} + H_2O} \qquad (1)$$

where (Cu)-O_2(ads) describes the undissociated O_2 molecule on the copper surface.

Also, the rate of the formation of [Cu(I)-BTA] film was suggested to be faster on the clean surface and in the presence of O_2 when compared to the formation on Cu_2O [32]. Furthermore, Chan and Weaver[22] suggest that the formation of the [Cu(I)-BTA] film takes place in atmospheric oxygen at open circuit potential and ambient temperature via half-reactions 2a and 2b:

Half reactions:

$$\mathrm{Cu + BTAH \Rightarrow Cu(I) - BTA + H^{+} + e^{-}} \qquad (2a)$$

$$\mathrm{O_2 + 4H^{+} + 4e^{-} \Rightarrow 2\ H_2O} \qquad (2b)$$

to produce the overall chemical reaction 3:

$$\mathrm{4\ Cu + 4\ BTAH_{(ads)} + O_2 \Rightarrow 4\ Cu(I) - BTA + 2\ H_2O} \qquad (3)$$

The opinion that oxygen is not needed in adsorption process has been supported for example by the studies of Fang *et al.*[17]. According to them the chemisorption of BTAH

molecules takes place also in the absence of oxygen and the hydrogen bonds between the C-H and N in the neighbouring BTAH molecules are suggested to cause the polymerization and the stability of the BTAH coating, as illustrated in Figure 1c. Furthermore, the adsorption of the first layer takes place in a similar way both on the clean and oxygen induced surfaces[17]. Tromans and Sun[31]have suggested that the adsorption of BTAH on oxygen-free surfaces depends on time and the potential in chloride containing solutions. Interestingly, they suggest that the formation of [Cu(I)-BTA] complex actually takes place in the solution, in the diffusion layer via $CuCl_2^-$ ions, and the polymeric film is formed when the complex adsorbs on this initial monolayer of BTAH on the Cu surface.

Recent theoretical calculations[27] also support the theory that oxygen is not necessary in adsorption process. Calculations of Jiang and Adams[27] predict that BTAH and BTA^- can either physisorb or even weakly chemisorb on a Cu(1 1 1) surface without oxygen and the polymerization of neighbouring BTAH/BTA^- molecules takes place by N-H…H bonds, as illustrated in Figure 1c. This gives rise to the following mechanism: a) BTAH/BTA^- is chemisorbed on the surface b) the next BTAH/BTA^- molecule is physisorbed to the surface and hydrogen bonded to the chemisorbed molecules by N-H…H bonds c) the next BTAH/BTA^- is again chemisorbed. When the calculations were done in the presence of OH^- ions it was found that two chemisorbed molecules were stabilized with C-H…H hydrogen bond. [27]

Some of the other studies, however, favour the assumption that BTAH adsorbs on the clean surface but oxygen enhances the adsorption and the film formation. For example, Ling *et al.*[26] suggest that the adsorption of BTAH is enhanced by Cu_2O on the surface and when the surface was etched prior to immersion the sample into a BTAH containing sulphuric acid solution (pH=2) the formation of the inhibitive layer did not occur. Also, Nilsson *et al.*[18] observed that the formation of [Cu(I)-BTA] was more pronounced on the thicker Cu_2O surfaces than on the thinner ones. Furthermore, Cho *et al.*[16] have observed that BTAH adsorbs on clean copper surface in a well-defined way and it can even form a multilayer (at least a bilayer) on the surface. When only a part of the

sample is exposed to oxygen, BTAH prefers the oxidised surface sites and oxygen seems to enhance the adsorption and the film growth. The adsorption on the oxidized surface was found to be more disordered and an amorphous film was grown on the surface.[16]

Plenty of studies have investigated the problem of whether oxygen is needed in formation of polymeric films. As majority of these studies involve "oxygen free atmospheres" produced simply by bubbling the solutions or cathodically reducing the surface without any further oxygen removal, the results must be treated with care: oxygen reacts with copper in milliseconds and the amounts needed for the formation of a cuprous oxide layer are very small.

2.3 Scanning Electrochemical Microscope (SECM)

SECM belongs to the family of scanning probe techniques and it was developed in the late 1980´s[33]. In SECM the current of an ultramicroelectrode (UME) (the electrode with the diameter of smaller than the diffusion layer[34]) is measured when it is held or moved in the electrolyte, proximal to the substrate of interest [33]. The solution contains redox species, called mediator, and its electrochemical reaction on UME, or a tip, is perturbed due to the nature of the substrate. Usually the size of tip is around 5-25 μm and the substrate can be either solid or liquid, its conductivity varying from ideally insulating to ideally conductive.[33] Hence, SECM has been found to be a very effective *in situ* tool for studying the nature and properties of different substrates. Moreover, commercial SECM also allows the potential control of the substrate. SECM has been used to study defects in aluminium oxide[35,36], redox active sites on titanium[37] and iodide oxidation at Ta/Ta_2O_5 electrodes[38] as well as utilised in corrosion studies[39].

In this Thesis the feedback mode of SECM has bee used to detect the formation of [Cu(I)-BTA] film on copper alloy surfaces as a function of alloying elements, substrate potential and oxygen content in the measurement environment.

2.3.1 Principles of Feedback Mode of SECM

In feedback mode of the SECM the steady state current of the tip is recorded as a function of the distance between the substrate surface and the tip. The movement of the tip in relative to the substrate is controlled by piezo elements in *x*, *y*, and *z* directions, *z* being the vertical direction. Mediator is oxidised on the tip causing the tip current and then reduced on the substrate surface. In this way a feedback loop between the tip and the substrate is established as illustrated in Figure 2 for the formation of an insulating [Cu-BTA(I)] film.

Positive feedback is observed as an increasing tip current while the tip approaches a conductive surface (Fig. 2a). Because the potential of the tip is selected so that the current of the tip is diffusion controlled, an increase in current is observed due to regeneration of the mediator at the conductive surface. When the substrate is insulating and the reduction of the mediator on the substrate surface is inhibited (Fig. 2b), the negative feedback is observed as a decrease in tip current when it approaches the surface. The decreasing current is due to the blocking effect of the tip because it hinders the diffusion field of the redox mediator surrounding the tip.

Using feedback mode the formation of a [Cu(I)-BTA] film can be detected as a function of time with SECM as the copper surface turns from almost ideally conductive to almost ideally insulating when the copper alloy is exposed to the solution containing benzotriazole.

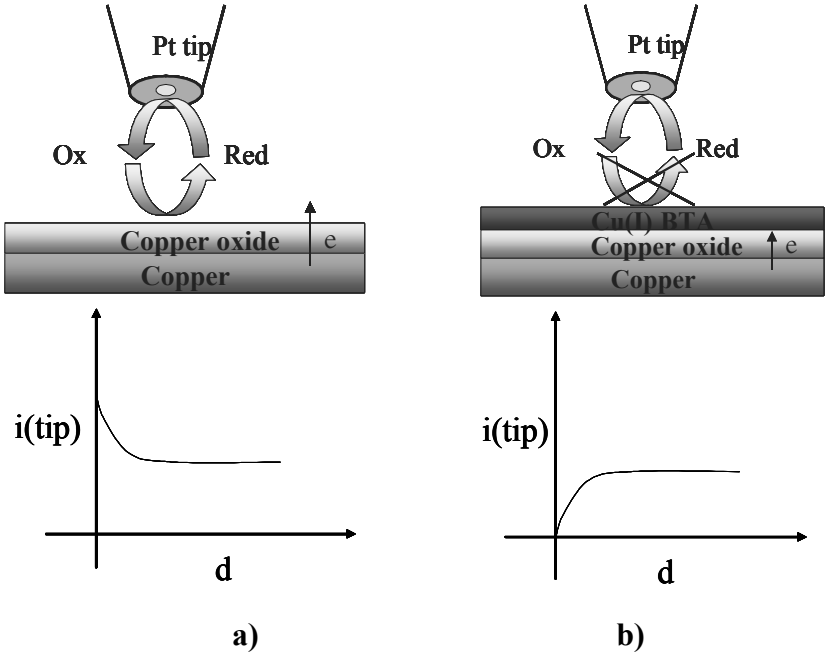

Figure 2. Schematic figure of the feedback mode of SECM: a) positive feedback, b) negative feedback. The positive feedback is recorded when the tip approaches conductive surface, in this case copper substrate and negative feedback when the tip approaches insulating surface, in this case [Cu(I)-BTA] film. d = the distance between the tip and the substrate, i(tip) = the current of the tip.

There are semi-empirical equations which can relate the current of the tip to the current of the substrate and they are introduced briefly below, starting from the general diffusion equation in the cylindrical coordinates. The theoretical discussion introduced below is based on the work of Bard, Mirkin and co-workers [40, 41] and it is used for modelling the SECM results introduced in this Thesis.

In general, the mediator is oxidised/reduced on the tip surface and re-reduced/re-oxidised on the substrate surface, according to Reactions 4 and 5, respectively:

$$R \rightarrow O + ne^- \quad (4)$$

$$O + ne^- \rightarrow R \quad (5)$$

Equation 1 introduces the time dependent diffusion problem of quasi-reversible mediator in cylindrical coordinates:

$$\frac{\partial C_\mathrm{i}}{\partial T} = \frac{\partial^2 C_\mathrm{i}}{\partial Z^2} + \frac{\partial^2 C_\mathrm{i}}{\partial R^2} + \frac{1}{R}\frac{\partial^2 C_\mathrm{i}}{\partial R} \qquad (1)$$

$$0 < T,\ 0 \le R,\ 0 < Z < L$$

$$R = r/a$$

$$L = d/a$$

$$Z = z/a$$

$$C_\mathrm{i} = c_\mathrm{i}/c_\mathrm{i}^\circ$$

$$T = tD_\mathrm{i}/a^2$$

where a = radius of the tip, r = radial coordinate, R = dimensionless radial coordinate, d = distance between the SECM tip and the substrate, L = dimensionless distance between the tip and the surface, z = vertical coordinate of the tip surface (normal), Z = dimensionless z coordinate, c_i = concentration of species i, c_R° = the bulk concentration of the reduced species of the mediator, C_i = dimensionless concentration of c_i, D_R = diffusion coefficient of reduced species of mediator, t = time. N.B. When the tip is held in the diffusion controlled potential region a steady-state condition can be applied ($\partial C_\mathrm{i}/\partial T = 0$).

The analytical approximations of diffusion equations for an irreversible, heterogeneous substrate kinetics (when $K_{\mathrm{b,S}}$=0) under the steady state conditions of the tip with associated boundary and initial conditions can be found from literature[40,41, 42] . The approximations are outlined in Equations 2-7 below.

Equations (2) and (3) give the dimensionless current of the tip, when the substrate is ideally insulating or ideally conductive, respectively:

$$I_\mathrm{T}^\mathrm{ins} = \frac{1}{0.15 + \frac{1.5358}{L} + 0.58\exp\left(\frac{-1.14}{L}\right) + 0.0908\exp\left(\frac{L-6.3}{1.017\cdot L}\right)} \qquad (2)$$

$$I_{\mathrm{T}}^{\mathrm{con}} = \frac{0.78377}{L} + 0.3315\exp\left(\frac{-1.0672}{L}\right) + 0.68 \tag{3}$$

'con' denotes a conductive and 'ins' an insulating substrate. The dimensionless current I_{T} is defined as:

$$I_{\mathrm{T}} = \frac{j_{\mathrm{T}}}{j_{\mathrm{T,lim}}} = \frac{j_{\mathrm{T}}}{4\mathrm{n}FDc^{\circ}a} \tag{4}$$

Where $j_{\mathrm{T,lim}}$ = the limiting diffusion current of the tip when it is far away from the substrate, n=the number of electrons changed in the reaction, F = Faraday's constant, D = diffusion coefficient of the mediator and $c°$ = bulk concentration of the mediator.

When the reaction at the substrate is under kinetic control, the dimensionless tip and substrate currents can be related by Equation (5):

$$I_{\mathrm{T}} = I_{\mathrm{S}}^{\mathrm{k}}\left(1 - \frac{I_{\mathrm{T}}^{\mathrm{ins}}}{I_{\mathrm{T}}^{\mathrm{con}}}\right) + I_{\mathrm{T}}^{\mathrm{ins}} \tag{5}$$

where

$$I_{\mathrm{S}}^{\mathrm{k}} = \frac{0.78377}{L\left(1 + 1/\Lambda\right)} + \frac{0.68 + 0.3315\exp\left(\frac{-1.0672}{L}\right)}{1 + \frac{11/\Lambda + 7.3}{\Lambda\left(110 - 40L\right)}} \tag{6}$$

'S' denotes the substrate and superscript 'k' kinetic control of the reaction. Λ is defined by Equation (7):

$$\Lambda = \frac{k_{\mathrm{f,S}}d}{D_{\mathrm{R}}} = K_{\mathrm{f,S}}L \tag{7}$$

where $k_{\mathrm{f,S}}$ is the rate constant of the forward reaction on the substrate surface and $K_{\mathrm{f,S}}$ is the dimensionless rate constant.

Furthermore, a rough estimate of the changes in the thickness of the film on the substrate surface can be also calculated as a function of time, if the thickness is assumed to be the only factor that influences the changes of the film resistance. In these cases the apparent $k_{f,S}$ can be defined as

$$k_{f,S} = \frac{D_{\text{film}}}{\delta} \tag{8}$$

where D_{film} is the diffusion coefficient inside the film and δ is the thickness of the film.

The modelling of SECM results in this Thesis is done according to Equations 2-8 using three parameters: (i) the distance between the tip and the substrate, *d*, (ii) the dimensionless heterogeneous rate constant of the reduction of the mediator at the substrate surface, $K_{\text{f, S}}$, and (iii) the limiting current i_{lim}. More details of the selection of these three parameters can be found in Publication I.

2.4 Studies of Inhibition of Copper Corrosion with Benzotriazole (Publications I-III)

The experimental work of the copper corrosion studies introduced in this Thesis has been performed using scanning electrochemical microscope (SECM). Also, electrochemical quartz crystal microbalance (EQCM) and x-ray photoelectron spectroscopy (XPS) have been used by co-authors of papers I and II further to complement SECM data but this Thesis concentrates mainly on SECM studies.

2.4.1 Effect of Potential and Alloying Element (Publications I and II)

Figure 3 shows an example of the SECM measurement of DHP copper as a function of exposure time to BTAH solution. In addition, the potential of the substrate (DHP copper) is kept constant: in Fig 3a it has been -0.05 V and in Fig 3b -0.20 V. The symbols are related to the experimental results while the solid lines are the modelling results. The effect of potential is clearly observed: at positive potentials the inhibitive film forms as a function of exposure time because the almost ideally conductive copper surface (positive feedback, increasing current) turns to almost ideally insulating one (negative feedback, decreasing current). In contrast, when the potential is changed to

-0.20 V the formation of the film is very slow and do not reach insulating properties even after four hours exposure.

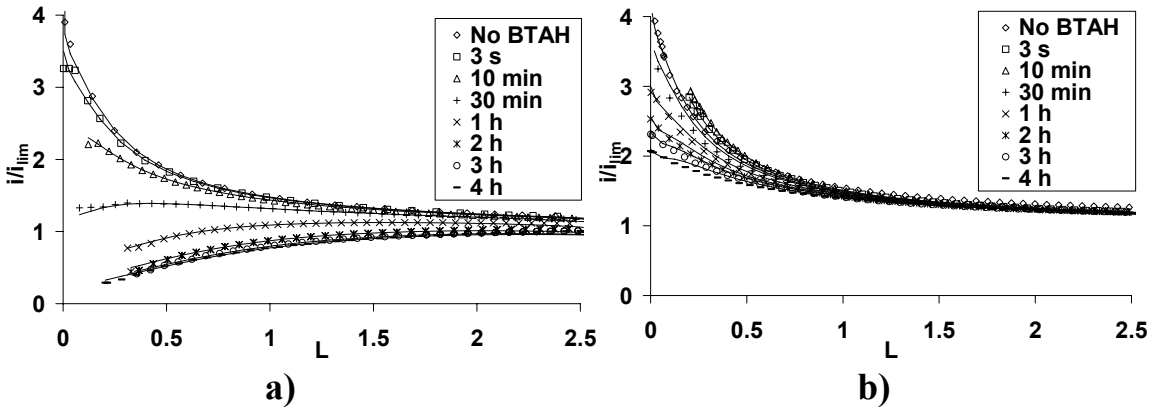

Figure 3. Approach curves as a function of exposure time measured at the substrate (DHP copper) potential of a) –0.05 V vs. SCE and b) -0.20 V vs. SCE. i/i_{lim} is the dimensionless tip current, and L = d/a is the dimensionless distance between the sample and the tip. Reproduced by permission of The Electrochemical Society.

These results are in good agreement with literature and the generalisation that the [Cu(I)-BTA] film only forms at positive potentials and at negative potentials the adsorption of BTAH molecules dominates. Only the change of the substrate surface from ideally conductive to ideally insulating is observed with SECM and the adsorption itself cannot be detected with this technique. Thus the distinction between adsorption of BTAH on the surface and formation of [Cu(I)-BTA] film is unable to be made. However, the literature is rather unanimous regarding the adsorption at the lower potentials and therefore it can be concluded that the adsorption of BTAH is not enough for the formation of an insulating surface but the formation of the [Cu(I)-BTA] film is needed.

Furthermore, the potentials at which the insulating film formation is still observed coincide with literature values; Chan and Weaver[22] have noticed that in acidic Na_2SO_4 solutions the formation of the [Cu(I)-BTA] film takes place at potentials more positive than -0.3 to -0.2 V vs. SCE and Youda *et al.*[21], on the other hand, suggest the film

formation takes place in neutral solution over the whole potential range but in acidic solution at potentials more positive than -0.3 V vs. SCE. SECM results presented here suggest that the potential range for the formation of the insulating film is from -0.2 V vs. SCE up to close to open circuit potential (OCP), depending on the alloying material (see below).

In addition to the matching potentials, the thickness values of the inhibitive films are in good agreement with literature. The thickness of the film is calculated using Equations 2-8 and with electronic diffusion coefficient inside BTAH film - $4 \cdot 10^{-9}$ cm^2/s. The calculated thickness values of the films as a function of potential after four hours exposure are shown in Table 1.

Table 1. The thickness values (δ) of [Cu(I)-BTA] film as a function of potential after 4h exposure for BTAH containing solution in a normal atmosphere. OCP values (open circuit potential) are given in parenthesis next to thickness values. The potentials are given as V vs. SCE.

Copper Alloy	**δ /nm OCP**	**δ /nm -0.05 V**	**δ /nm -0.10 V**	**δ /nm -0.15 V**	**δ /nm -0.20V**	**δ /nm -0.30 V**
OF-HC	27.8 (0.03V)	35.5	--	--	19.7	--
DHP	--	29.6	3.2	4.3	2.9	1.7
CuAg	0.9 (0.05V)	0.9	--	--	0.9	--

As can be seen, for example for OF-HC the values are around 20-35nm, depending on the potential of copper substrate. The values found in literature are quite similar: for instance, according to Brusic *et al.* [15], the film thickness is around 1-4 nm after 10-30 min immersion and according to Metikoš-Huković, Babić and co-workers[2, 43] it is around 10-20 nm. Frignani *et al.*[44], who have also performed the measurements in Na_2SO_4 solution, have estimated the thickness values between 1-18 nm after three hours exposure.

It has to be remembered, though, that the calculated thickness values are only rough estimates due to the simplifications made in Equation 8 which assumes that only

diffusion of ions/electrons is relevant and for example no migration can take place. Furthermore, the estimation of the electronic diffusion coefficient from ionic diffusion coefficient inside [Cu(I)-BTA] film is done using a model which is developed for oxide layers on metal surfaces[45, 46]. Thus, the approximation from the ionic diffusion coefficient to electronic diffusion coefficient is not accurate and the final thickness values must not be treated as exact values but merely they should to be seen more as a way to compare results of different SECM measurements. Nevertheless, as the estimated thickness values are in the same range as those in literature the assumptions in the calculations can be deemed to be acceptable.

Figures 4a-b show the approach curves of OF-HC at potentials -0.05 V and -0.20 V, respectively. The same effect of potential is observed again even though in the case of DHP copper (Fig 3) the trend is more pronounced because on the OF-HC copper surface the film grows at a slower rate at -0.20 V than at -0.05 V but it still displays insulating behaviour after 2 hours exposure.

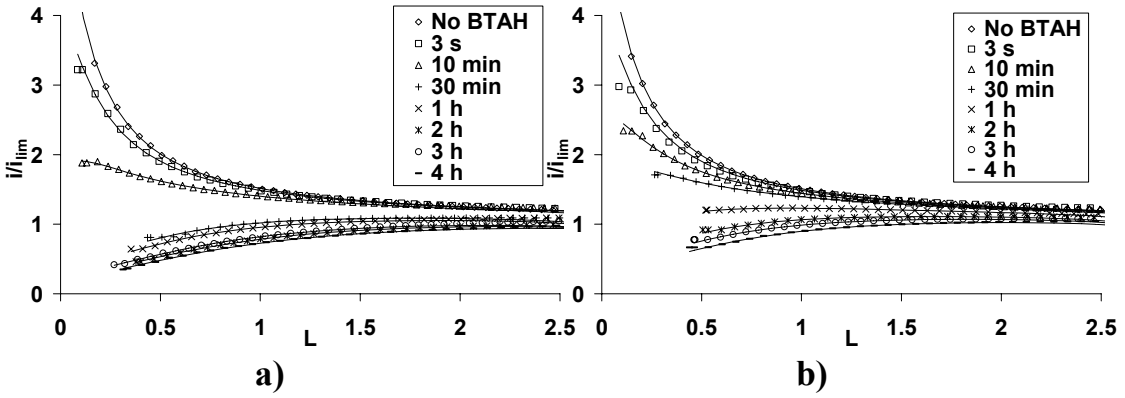

Figure 4. Approach curves as a function of exposure time measured at the substrate (OF-HC) potential of a) –0.05 V vs. SCE and b) -0.20 V vs. SCE. i/i_{lim} is the dimensionless tip current, and L = d/a is the dimensionless distance between the sample and the tip. Reproduced by permission of The Electrochemical Society.

When these figures are compared to Figures 5a-b, which introduce the approach curves of CuAg at -0.05V and -0.20 V, respectively, an interesting phenomenon is observed:

the inhibitive film does not grow on the surface of CuAg copper at all and this behaviour is independent of the potential. Furthermore, a comparison of the approach curves for all the studied material measured at -0.05 V (Figs 3a, 4a and 5a) it can be clearly seen that with the purest material, OF-HC, the formation of the film is fastest and occurs within an hour whereas in the case of copper alloyed with phosphorus (DHP) the formation is a bit slower. This strong effect of the alloying component on the formation of [Cu(I)-BTA] has not been previously observed.

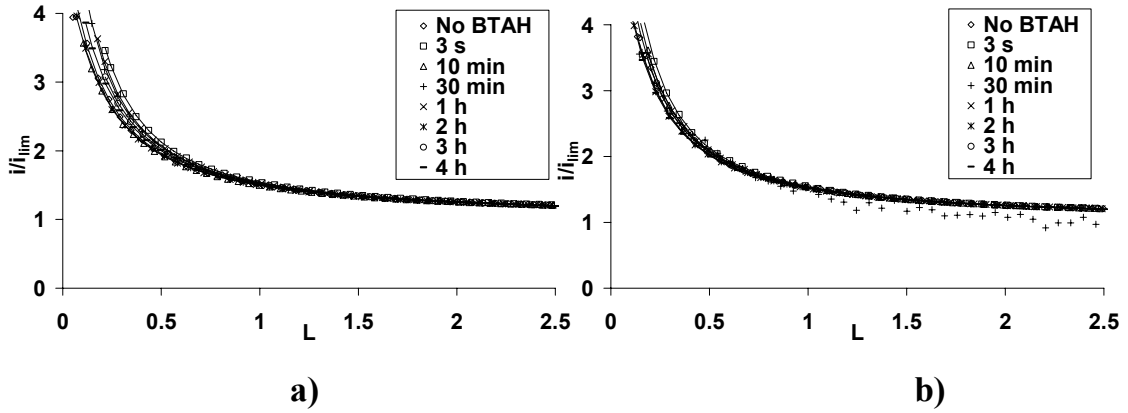

Figure 6. Approach curves as a function of exposure time measured at the substrate (CuAg, Ag>2%wt) potential of a) –0.05 V vs. SCE and b) -0.20 V vs. SCE. i/i_{lim} is the dimensionless tip current, and L = d/a is the dimensionless distance between the sample and the tip. Reproduced by permission of The Electrochemical Society.

The SECM results prove that no inhibitive [Ag(I)-BTA] film can form inducing that silver as an alloying component hinders the formation of [Cu(I)-BTA] film. Moreover, during the electropolishing step, the silver amount on the surface probably increases due to selective dissolution of Cu resulting in Ag rich surface. This is illustrated by SECM measurements performed with non-electropolished CuAg that show the formation of the inhibitive film (Publication II, Figure 7). XPS results made by co-authors (Publication II, Figures 8-12) further enhance this hypothesis as no change in Ag spectra is observed after exposure to BTAH solution, indicating no Ag-BTAH interaction.

2.4.2 Effect of Oxygen (Publication III)

Figures 6a-c show the effect of oxygen on the formation of the inhibitive film on OF-HC copper surface, at open circuit potentials when the oxygen level is O_2 = normal atmospheric conditions, O_2 = 25-75ppm or O_2 = 0-15ppm, respectively.

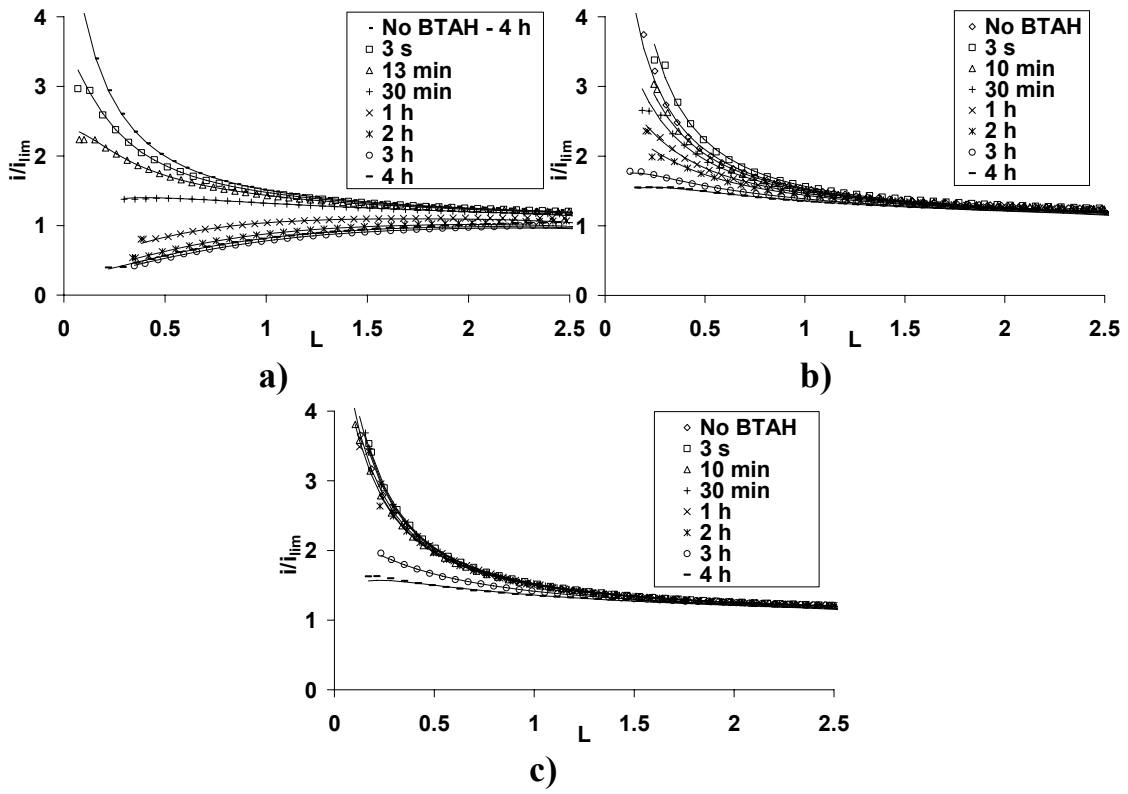

Figure 6. Approach curves to OF-HC copper as a function of exposure time to BTAH measured at open circuit potential at oxygen content a) normal atmospheric conditions, b) 25-75 ppm, c) 0-15 ppm. i/i_{lim} is the dimensionless tip current, and L = d/a is the dimensionless distance between the sample and the tip. Reproduced by permission of The Electrochemical Society.

In a normal atmosphere, without the BTAH exposure, the copper surface stays ideally conductive even after four hours as the first approach curve in Fig 6a shows. However, immediately after the sample is exposed to BTAH solution the formation of the inhibitive film starts and it is seen as a decreasing current with increasing exposure

time. Almost ideally insulating behaviour is reached within an hour (Fig 6a). When the atmospheric oxygen level is decreased to 25-75 ppm (Fig 6b) the formation of the film is much slower and during the whole exposure time the film does achieve totally insulating behaviour. When the oxygen content is reduced even further to 0-15 ppm (Fig 6c), the formation of the film is completely absent for the first 2-3 hours after which only a slight decrease in the current is observed.

These experiments clearly indicate that oxygen is needed for the formation of an inhibitive [Cu(I)-BTA] film. Also, the results are strong evidence for the capability of atmospheric/dissolved oxygen promoting formation of inhibitive film because the slow formation of the inhibitive film (Fig6c) is believed to be due to residual oxygen in a solution rather than the remaining cuprous oxide on the surface. This is because there is no sign of formation of the inhibitive film during the first few hours as would be the case if some cuprous oxide was still be on the surface. It is not, however, entirely verifiable and consequently the possibility of a three step process including 1) diffusion of O_2 to the surface, 2) reaction with copper to copper oxide, and 3) the reaction of solid copper oxide and BTAH to [Cu(I)-BTA] film, cannot be excluded. Nevertheless, also the XPS results in Publication II imply that formation of [Cu(I)-BTA] film takes place with parallel dissolution of copper ions from the surface and thus also the mechanism with dissolved oxygen is probable, in a similar fashion to Reactions 1 and 2 outlined earlier in Section 2.2.

2.5 Summary of Inhibition of Copper Corrosion Studies

SECM has been proved to be an efficient tool in observing the formation of insulating film on the conductive surface. The formation of [Cu(I)-BTA] film has been studied with three different copper alloys, OF-HC, DHP and CuAg, and significant differences can be found in the formation of the insulating benzotriazole film on these materials. The film grows fastest on the OF-HC surface and surprisingly, no inhibitive film is

detected on CuAg surface. This is believed to be due to the enrichment of Ag on the surface during the electropolishing step.

In addition, potential has been found to have a crucial effect on the formation of the Cu(I)-BTA film and even if some adsorption would take place at negative potentials (lower than ~ -0.20V vs. SCE) the formation of the film only takes place at more positive potentials (closer to the OCP). Furthermore, the effect of oxygen has been studied in this Thesis and the SECM results clearly show that oxygen is needed for the formation of [Cu(I)-BTA] film.

3 Surface Modifications with Silver Nanoparticles

The second part of Thesis – surface modifications with silver nanoparticles - is outlined in this chapter. Firstly, surface modifications with sol-gel films which contain silver nanoparticles are discussed. Secondly, the new approach for the synthesis of tightly bound silver nanoparticles in ultra-thin films is introduced.

Several physical properties of materials – especially optical and electronic - alter from their bulk properties when the physical size of the material is reduced to nanometer scale (≤ 100 nm).[5] Currently, "nanoparticle" as a concept is used to describe quite a wide variety of different types of materials with different sizes – for example, the size of so called solid-lipid nanoparticles can be up to 700 nm[47] while in some cases, nanoparticle is taken as a quantum dot with a size up to few nanometres[48]. In this Thesis, the concept of nanoparticles is used to describe metallic particles in a solution or metallic inclusions inside films. Although their size distribution is allowed to be rather wide the largest dimension is, however, less than 50 nm and the smallest few nanometres.

The synthesis of metal colloids has been studied for decades[5] but the controlled synthesis of nanoparticles has opened a wide range of possibilities for their use in applications. The most common synthesis methods are the reduction of metal salts in the presence of citrate anions developed by Turkevich and co-workers[49], two-phase reduction synthesis developed by Brust, Schiffrin and co-workers[50] and the inverse micelle method combined to size selective precipitation introduced by Pileni and co-workers[51]. A number of modifications to these methods have also been subsequently developed.

3.1 Applications of Ag Nanoparticles

Due to their interesting properties, nanoparticles allow a very fascinating approach for surface modifications. Even small amounts of nanoparticles on the surface can bring new functionalities into the material such as antibacteriality [52] or catalytic activity[53]. The main difficulties lay with the attachment of nanoparticles on the surface in such a way that their functionalities are not lost but the film is stable on the surface. In addition, the attachment of nanoparticles has become an increasingly important factor due to their unknown health risks.

Therefore, the focus of this Thesis is on the surface modifications with Ag nanoparticles by improving the properties of the nanoparticle films on surfaces (sol-gel films, Sections 3.2-3.3) and development of a new, *in situ* way to introduce tightly bound nanoparticles on the surface of interest (ultra-thin films, Sections 3.4-3.5). Silver nanoparticles have been selected to be studied material due to their wide range of applications. Some of them are briefly outlined below.

3.1.1 Antibacterial Properties of Silver

Ag^+ ions have been utilised for medical purposes for several centuries[54], [55] and also Ag nanoparticles have shown antibacterial properties [6, 56, 57]. Whether the nanoparticle itself or the release of Ag^+ ions causes the antibacterial effect is, thus far, not clearly understood and in some cases, not even discussed.

The mechanism of the antibacterial processes of silver in different forms has caused some interest.[6, 58, 59,60] In general, antibacterial activity of silver ions is believed to be due to the interaction with thiol or other sulphur containing groups in the bacterial membrane causing the death of the microbial cell. It has been suggested that only silver ions have antibacterial effects and even the presence of accompanying anion like NO_3^- reduces its effectiveness.[58] Lok *et al.*[60], on the other hand, suggest that Ag nanoparticles

in a solution target the bacterial membrane and actually, their mechanism is quite similar to as silver ions in $AgNO_3$ solution.

Antibacterial properties have been observed on substrates modified with silver nanoparticles[6, 56, 57]. Panáček *et al.*[6], for example, have studied the antibacterial activity of silver colloids with different size distributions. Even though the mechanism is not clearly understood, they suggest that the permeation and respiration of bacteria is destroyed by the attachment of silver nanoparticles to the surface of cell membrane. They emphasize that silver nanoparticles have not only an inhibitive effect on the growth of bacteria but they have also the killing ability. It is worth noting that although the permeation of silver nanoparticles is possible the release of silver ions is not excluded either.[6] Dai and Bruening[56] have been able to create antibacterial films containing Ag^+ ions and Ag nanoparticles. According to them, nanoparticle loaded films are preferable as they reduce the harmful diffusion of Ag^+ ions into the body.[56] Furthermore, Shi *et al.*[57] have detected the enhancement of the antibacterial properties of N-hexyl-N-(4-vinylbenzyl)-4,4'-bipyridium dinitrate (HVVN) films when silver ions are reduced by UV irradiation to Ag nanoparticles inside them.

Rubner, Cohen, and co-workers[61, 62], on the other hand, suggest that silver ion rather than the nanoparticle itself is the killing substance. However, nanoparticles posses a slower release of Ag^+ ions and the rate determining step is the oxidation of zerovalent Ag, not the diffusion of silver ions in the film[61]. They have also developed coatings that have two levels of antibacterial capacities, so called ´chemical releasing bacteria-killing´ and ´contact bacteria-killing´ capacities. The ´chemical releasing bacteria-killing´ capacity is obtained with the dissolution of silver ions to the surrounding environment. The 'contact bacteria-killing capacity' is achieved by the silica nanoparticle cap with quaternary ammonium salts which are known of their ability to ´contact-killing´ mode due to their fatty alkyl chains. [62] Recently, a simple method to incorporate silver nanoparticles homogeneously into a titanium phosphate multilayer matrix using ion-exchange processes with Ti^+ and Ag^+ ions was introduced by Wang *et al.*[63] and these types of films also showed antibacterial properties.

3.1.2 Raman Scattering and SERS Activity of Silver

Raman scattering was first introduced by Raman and Krishnan in 1928 who observed that when liquid was radiated with an incident of light an inelastic, scattered light was observed to radiate from the surface.[64] The enhancement of Raman spectra of pyridine by silver was first observed by Fleischmann and co-workers in 1974[65, 66] and since then there has been an active discussion as to the mechanism of the Surface-Enhanced Raman Scattering (SERS).

Two explanations -electromagnetic enhancement and chemical enhancement- are nowadays accepted to explain SERS activity.[67, 68] Both of these explanations require the involvement of what are known as active sites. The increased coupling between the adsorbate molecule and the noble metal takes place at the chemical active sites. On the other hand, the electromagnetic active sites are believed to result in interactions of the electromagnetic fields between the noble metal nanoparticles and matrix (local field effects which are due to the difference in dielectric constants of the matrix and the quantum dots). [68] Recently so called single molecule SERS (smSERS) has even further increased the interest in the field[69] and SERS active surfaces containing nanoparticles have undergone intensive development [7, 70, 71].

3.1.3 Optical Switches

In addition to antibacterial properties and SERS activity, the incorporation of silver nanoparticles into a silica coating – for example via sol-gel route or ion-exchange methods- has been studied due to their ability to enhance non-linear optical phenomena, allowing its use for example as an optical switch with time scales of less than picoseconds.[72], [73]

In general, non-linear electromagnetic phenomena occur when a material responds to changes in the amplitude of applied electronic and magnetic fields in a non-linear manner[74]. If a material possesses an optical non-linear susceptibility (such as glass) the

refractive index and absorption of the material are changed while light passes through them and also, the light itself is affected by this change in a non-linear way. It has been found that the third-order optical non-linear susceptibility, $\chi^{(3)}$, of a glass can be enhanced by several orders of magnitude by incorporating metal colloids and nanocrystals inside the glass. The third-order optical non-linear susceptibility is related to the non-linear portion of the refractive index of the material, which, in itself, is proportional to the intensity of light. Thus the switching can be accomplished by changing the intensity of light. [72]

Due to aforementioned properties of silver, the surface modifications are carried out with Ag nanoparticles. Both more traditional sol-gel coatings and newly developed ultra-thin films have been studied in this Thesis and they are discussed in Sections 3.2-3.3 and 3.4-3.5, respectively.

3.2 Background to Sol-Gel Films with Ag Nanoparticles

Surface modification with sol-gel coatings is, by no means, a novel technology. The first sol-gel process –even though only an accidental one - was reported already in 1846 by Ebelmen[75] but it took until 1939 before it was realised that the formation of SiO_2 film could be achieved by using alkoxides[76, 77, 78] Since the 1950's there has already been industrial use of specific sol-gel coated applications to produce things like rear view mirrors, antireflective and solar-reflective coatings. In the late 1960's and early 1970's the discovery of metal(I)-oxygen-metal(II) formation allowed the production of glass-ceramics, crystalline layers and multi-component oxide glasses and thus widened the area of applications.[78] More recently, nanoparticles have been introduced into the sol-gel coatings resulting in the thin, homogenous coatings with the special functionalities of nanoparticles[8].

The advantage in using sol-gel coatings is that it provides a cheap, simple and versatile way for the silica matrixes to form with adhesive bonding between the surfaces[79]. First,

a sol is formed of the colloidal suspensions containing solid particles and polymers[77, 80] and later the gelation takes place resulting in a sol-gel[80]. The films can be prepared at low temperatures and by selection of chemicals and pH, the formation can be easily tailored to different applications. Building the inorganic network of sol-gel coating demands hydrolysis and condensation polymerisation reactions, which can be summarised in Reactions 6-8 [8, 77, 81]:

$$\mathrm{Si(OR)_4 + H_2O \rightarrow OH - Si(OR)_3 + ROH} \quad (6)$$

$$\mathrm{(OR)_3Si\text{-}OH + OH - Si(OR)_3 \rightarrow (OR)_3Si\text{-}O\text{-}Si(OR)_3 + H_2O} \quad (7)$$

$$\mathrm{(OR)_3Si\text{-}OR + OH - Si(OR)_3 \rightarrow (OR)_3Si\text{-}O\text{-}Si(OR)_3 + ROH} \quad (8)$$

The hydrolysis of alkoxysilane precursors is outlined in Reaction 6 whilst Reaction 7 shows the condensation polymerisation between the hydrolysed species. Reaction 8 displays the polymerisation condensation between the alkoxy group and hydrolysed species that results in the inorganic backbone of the coating.[80]

Silver doped silica coatings can be easily prepared using tetraethyl-orthosilicate (TEOS), $AgNO_3$ and HNO_3 as the main precursors[82, 83, 84] and the use of functionalised silanes allows the anchoring of Ag nanoparticles to the host matrix to be readily achieved[80]. Amino silanes have been found to be suitable stabilisers for Ag nanoparticles in sol-gel coatings[84]. There are several possible routes to obtain Ag nanoparticles inside the silica like coating and for example, thermal treatment up to 600°C either in air[82, 83] or in reducing atmosphere[84, 85] has been used widely. Additionally, the use of UV curing[86] or γ radiation of mesoporous silica immersed in Ag^+ solution[87, 88] have been reported to form nanoparticles inside the coating.

The effects of heat treatment on the formation of Ag nanoparticles have been subject of intense study [83, 84, 85, 89, 90]. In general, some nanoparticles are observed to form during the drying process at 60-120°C in air but higher temperatures up to 350°C enhance the precipitation of nanoclusters and nanoparticles. Interestingly, further heat treatment

between 400-600°C in air results in the disappearance of silver clusters and the yellow colour of the coating whilst the re-introduction of particles is observed at higher heat treatment temperatures (500-800°C) or in the reducing atmosphere. The reason for this type of observation has been widely discussed and it is commonly believed that such a behaviour is due to formation of silver oxide at the intermediate temperatures[83, 84, 85, 89] although aggregation/disaggregation of nanoparticles has been proposed as an alternative hypothesis[90].

Additionally, the stability of the coatings in light has caused debate.[82, 91] As a general rule, nanoparticles prepared by low temperature heat treatments (below 500°C) are not stable in light and air while the stability is increased when the treatment is performed at higher temperatures (up to 800°C). Jeon *et al.*[82] have suggested that the instability of the low heat treated samples is caused by the incomplete trapping of Ag^{+} ions in the silica matrix and Shibata *et al.* [91] propose that the monodisperse, high temperature treated samples are more stable.

Overall, despite of the huge amount of synthetic work done in the field, the detailed chemistry between the nanoparticles and the matrix remains unsolved. This is especially true when considering the blueshift of the Surface Plasmon Resonance peak (SPR) which has been observed together with the growth of particle size even though blueshift is commonly related to the decrease in particle size.[88, 92] Such a contradictory behaviour is related to the interactions between the particles and silica matrix. For example, Pan *et al.*[88] suggest that before annealing the pores of the SiO_2 matrix are large when compared to particles and thus the size effect dominates. Annealing, however, increases particle size, thus the interaction with the surrounding matrix becomes more predominant. [88]

3.3 Studies of Silver Nanoparticle Containing Sol-Gel Films (Publication IV)

This thesis introduces a facile sol-gel synthesis for silver nanoparticle coatings. The stability of the coatings has been investigated and further modifications of the coatings have been carried out by oxidising and reducing low temperature plasma treatments.

3.3.1 Effect of Plasma Treatments on Nanoparticles and Matrix

When sol-gel films containing silver nanoparticles are exposed to the natural light and air, four characteristic changes are observed in the UV/Vis spectra (Figure 7a): 1) the absorbance of the Surface Plasmon Peak (SPR) related to the Ag nanoparticles decreases, 2) the position of the peak is redshifted, 3) the shape of the peak is broadened and 4) an increase in absorbance is observed in the range 600-800 nm during the exposure. These results clearly show the unstable nature of the film.

In an effort to increase stability, the sample was treated with low temperature O_2 plasma (which is known to calcinate the silica matrix) and the stability in light and air was subsequently studied with UV/Vis (Figure 7b). It can be observed that after O_2 plasma treatment both the absorbance and the width of SPR peak are nearly constant during the 24 hours exposure to air and light whilst the position of the peak is redshifted in a similar manner to untreated sample.

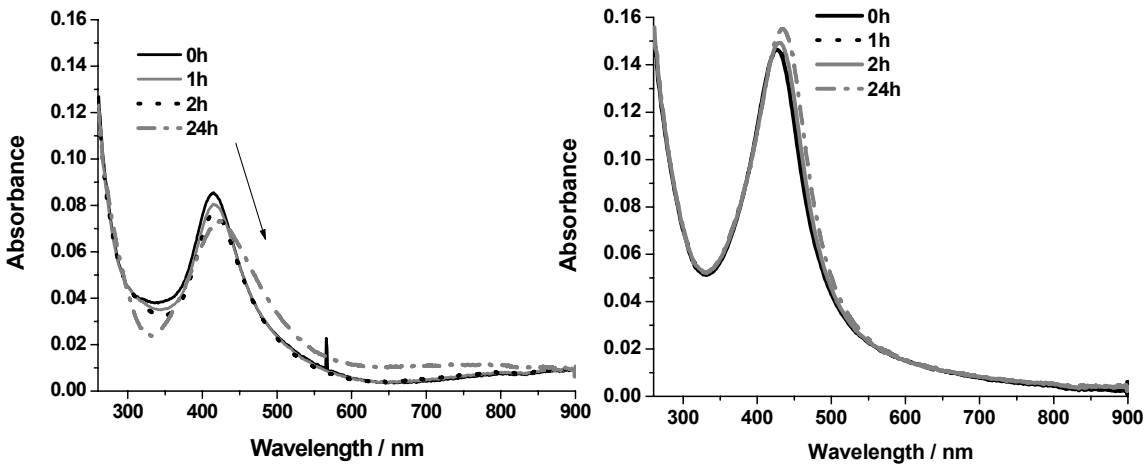

a) *b)*

Figure 7. UV/Vis spectra of sol-gel films containing Ag nanoparticles as a function of exposure time in air and light: a) no plasma treatment and b) after 10 min O_2 plasma treatment. Reproduced by permission of Elsevier B.V.

Further treatment of the sample with H_2 plasma was performed for the film and the effect of the plasma treatments was studied (Fig 8). It can be observed that O_2 plasma treatment decreases the absorbance, slightly broadens and changes the position of the SPR peak when compared to the untreated sample. H_2 plasma treatment, on the other hand, increases the absorbance and decreases the peak width to the original level. The centre of the peak, however, remains at a similar wavelength as that observed after O_2 plasma treatment.

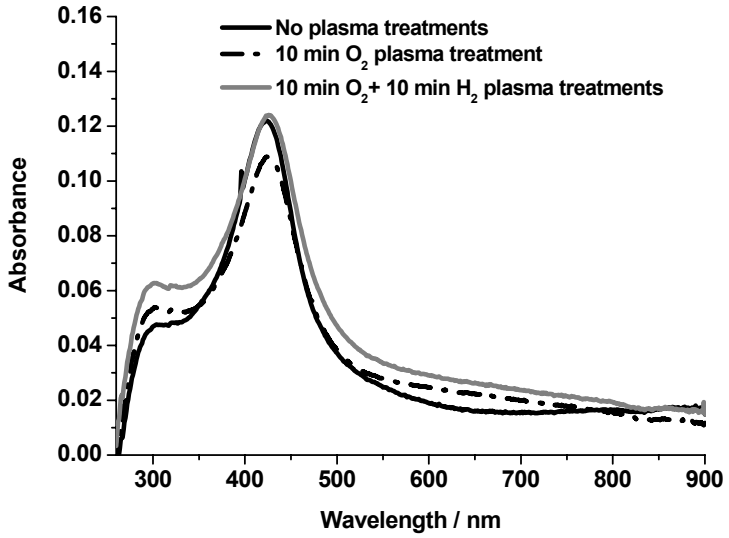

Figure 8. UV/Vis spectra of sol-gel films containing Ag nanoparticles as a function of exposure time in air and light with no plasma treatment, 10 min O_2 plasma treatment and 10 min O_2 + 10 min H_2 plasma treatments. Reproduced by permission of Elsevier B.V.

Even though some self-healing of the matrix is believed to occur during the H_2 treatment, FT-IRRAS data (Figure 5 in Publication IV) show that the changes in the matrix mainly take place during O_2 plasma treatment and H_2 plasma treatment does not result in dramatic matrix changes anymore. Therefore, the broadening of the peak and the decrease in absorbance are related to the changes in nanoparticles rather than in matrix because they occur even after H_2 plasma treatment. In addition to calcination of the film, O_2 plasma treatment is also believed to oxidise some of the nanoparticles or create an oxide shell on the nanoparticle surface, which leads to the decrease in absorbance and broadening of SPR peak. The increase in the absorbance of SPR peak observed during the reducing H_2 plasma, on the other hand, is due to re-reduction of the nanoparticles.

Additionally, electrochemical impedance spectroscopy (EIS) data (Figures 10-11 in Publication IV) show that also the presence of nanoparticles inside the matrix have an

enormous effect on the barrier properties – probably due to physical barrier they create in the conductive pathways – in borate buffer solution after O_2 and H_2 plasma treatments.

The hypothesis introduced above is enhanced by ToF-SIMS studies (Figure 4 in Publication IV) which show an increase in the O content after O_2 plasma treatment and then a return to a more normal O content after H_2 treatment. Furthermore, the formation of an oxide shell on Ag nanoparticles during the O_2 plasma treatment would explain also why no changes in absorbance or in the shape of the peak are observed after O_2 plasma treatment when the sample is exposed to light and air.

The reason for the change in the position of the peak, on the other hand, could be explained by the excess of Ag^+ ions which are believed to be still present in the matrix after drying at 120°C (similar to observation of De *et al.* [83]). Ag clusters and the excess of Ag^+ ions may react with the amino and silanol groups of the matrix during the exposure to air and light as suggested by Jeon *et al.*[82]. This would lead to the observed redshift in the peak centre. Such a hypothesis is further enhanced because the position of the SPR peak remains the same after O_2 and H_2 plasma treatments. The suggested hypothesis of the effects of the plasma treatments is illustrated in Figure 9.

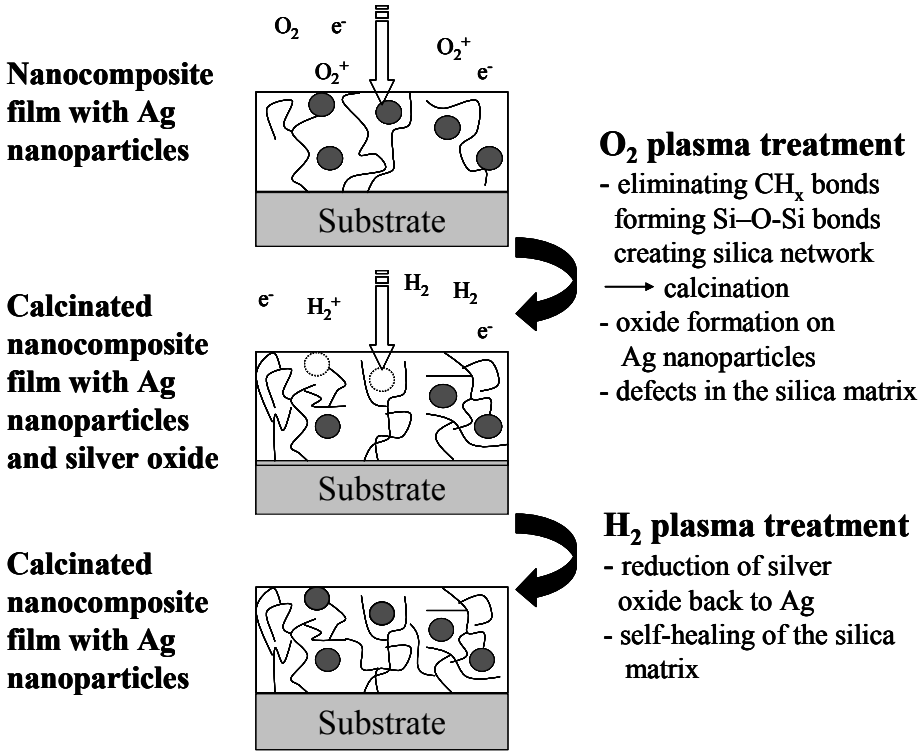

Figure 9. Schematic model of the effect of plasma treatments on sol-gel films containing Ag nanoparticles. Reproduced by permission of Elsevier B.V.

3.4 Background to Ultra-Thin Films

As the previous section showed, the work carried out in the sol-gel field is intensive and the benefits of the sol-gel based coating methods is the ability to produce high purity, homogenous films at low cost and which can be easily tailored and processed at low temperatures. However; subsequent processing – moulding, cutting, etc. - is almost impossible for materials modified with sol-gel because such films easily undergo a mechanical break-down. Additionally, sol-gel films are rather thick and thus the inherent characteristics of the original surface are changed, e.g. colour and conductivity. Therefore, a new approach for surface modification has to be developed as several applications demand that the original properties are maintained, either for aesthetic reasons (such as stainless steel kitchen equipment) or for the conductance reasons as is case for electronic applications.

Furthermore, along with the development of new applications that contain metallic nanoparticles there is also increasing concern as to the possible health risks posed by nanoparticles if dissolved into the surrounding environment [9, 10] Hence, there is an urgent requirement for surface modifications in which the nanoparticles are tightly attached to the surface. On the other hand, this raises the question as to whether such tight attachment of nanoparticles to a surface will compromise their capacity as an antibacterial material.

In this Thesis, a novel way to produce tightly bonded Ag nanoparticles on a surface is introduced where the nanoparticles are formed on the surface *in situ*. This method - similar to the Layer-by-Layer (LbL) technique- results in ultra-thin, almost invisible films to the naked eye. The interesting question is if the films really posses their antibacterial nature despite of the tight bonding of nanoparticles on the surface. In addition, SERS activity of silver outlined earlier is believed to take place using so called hot particles[69]. It has been estimated by Kneipp *et al.*[93] that only small amount of particles present are responsible for the observed enhancement. This could cause problems when ultra-thin films containing extremely small amount of Ag on the surface are in question. Therefore, also the antibacterial properties and SERS activity of the films has been studied in this Thesis.

The research of Layer-by Layer (LbL) type films has been extensive, starting with the work on bilayer assemblies of chlorosilanes via sequential chemisorption and activation of the organic molecules for further chemisorption by Netzer and Savig[94] and Zr-organic multilayers developed by Mallouk and co-workers[95,96]. The first layer has to be covalently bonded to the surface and silanols have been found to be suitable for this purpose. The deposition of the next layer usually requires either the activation of the first layer, i.e. modifying the heads of organic molecules so that the next layer can covalently bond to them, or the finding another molecule which can directly react with the pre-existing layer. The advantages of this technique are the versatility and the possibility to control the growth of the film on the monolayer level. In addition, the

layers are easy to build up as they need only a dipping or immersion of the sample into the solution of interest. For example, long-tailed organosilanes have been found to form well-structured multilayers on silicon surfaces when they are prepared using the LbL technique and the CH_3 head of the silanes is alcohol terminated to allow the attachment of the next layer[97]. Both a small average degree of interlayer polymerisation and a small fraction of interlayer covalent bonds are observed. Studies in this particular area and that of metal nanoparticle incorporation has been considerable [57, 61, 62, 98, 99, 100, 101, 102, 103, 104].

3.5 Studies of Ultra-Thin Films (Publication V)

This communication introduces a very facile route to prepare ultra-thin films directly on the surface of interest. Also, the SERS and antibacterial activity of the films which contain tightly bound silver nanoparticles was studied. In addition to the tight attachment of the nanoparticles the advantages of the ultra-thin films are the straight-forward nature of the synthesis and thus also the simplicity of the film chemistry. This in turn leads to reduction in the number of chemicals and finally, as the films are very thin, the original colour of the underlying surface can be maintained. When compared to the LbL method that uses the pre-prepared nanoparticle colloids, the new approach introduced here further simplifies the processes. Additionally, the need for any further reducers like $NaBH_4$ or H_2 is removed by the use of the amino functionalised trimethoxy silanes which promote both the attachment to the surface and the reduction of the nanoparticles during annealing.

3.5.1 Formation of the Ultra-Thin Films

A simple synthesis for ultra-thin films containing silver nanoparticles has been developed by the author and consists of three steps: Step 1) clean samples are exposed to DIAMO for 24h and then rinsed carefully with Methanol and dried by a stream of N_2. Step 2) Samples are subsequently dipped for 24h into the solution of 0.50g $AgNO_3$ +

20ml MeOH, which had been stirred for an hour prior to use. After 24h the samples are carefully rinsed again with MeOH and dried with N_2. Step 3) Finally, the samples are annealed in air at 120°C.

The formation of Ag nanoparticles during the annealing step (Step 3) can be clearly observed from UV/Vis spectra of glass and stainless steel samples (Figures 10 and 11, respectively) because the growth of SPR peak around 400 nm can be detected as a function of annealing time. Surprisingly, the formation seems to take place in a similar manner on both the insulating and conductive surfaces suggesting that the nature of the surface does not play a crucial role in the formation of the Ag nanoparticles. In fact the polymerisation of DIAMO molecules on the surface during the annealing step is believed to be responsible for the formation of nanoparticles.

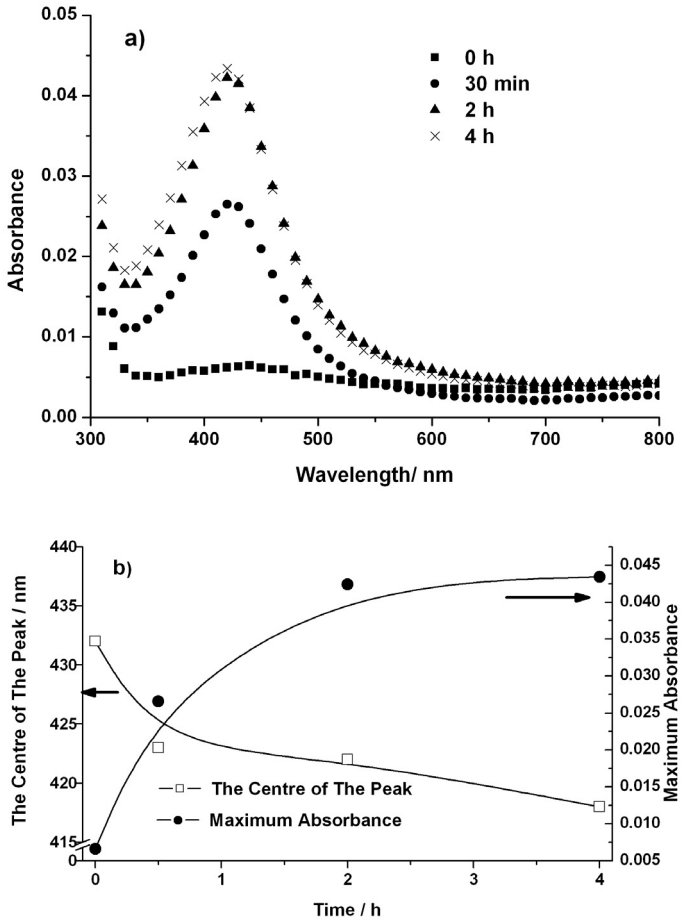

Figure 10. a) UV/Vis spectra of ultra-thin films on glass substrate as a function of annealing time. b) Centre of the peak and maximum absorbance in UV/Vis spectra as a function of annealing time. The solid lines are only for visualisation purposes. Reproduced by permission of The Royal Society of Chemistry.

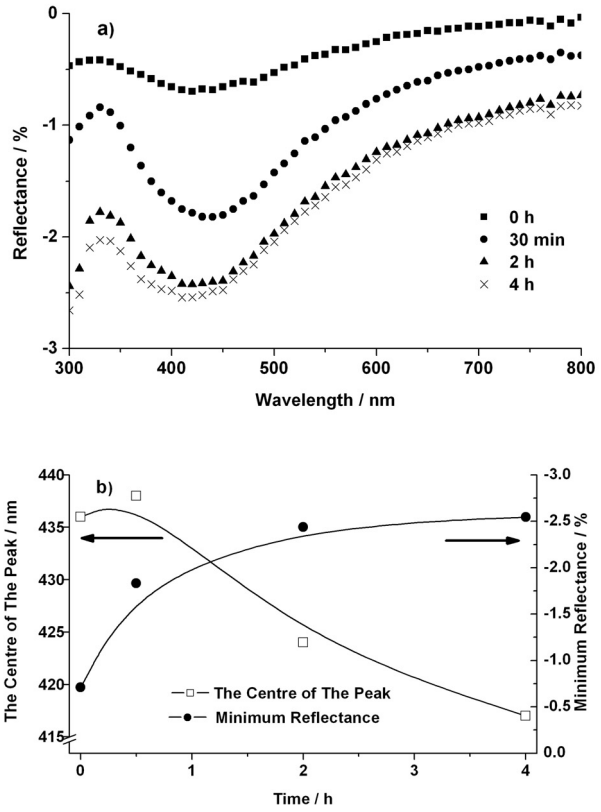

Figure 11. a) UV/Vis spectra of ultra-thin films on stainless steel substrate as a function of annealing time. b) Centre of the peak and minimum reflectance in UV/Vis spectra as a function of annealing time. The solid lines are only for visualisation purposes. Reproduced by permission of The Royal Society of Chemistry.

When the stainless steel samples are studied before and after the annealing step (annealing: at 120°C for 2h) by SEM and AES (Figures 3 and 4 in Publication V, respectively) it can be observed that large Ag containing clusters are formed during the immersion into the $AgNO_3$ solution. After the annealing silver is distributed more homogenously on the surface and only small Ag islands are observed in both the SEM and FE-AES images. Therefore, these results enhance the theory that Ag nanoparticles form during the annealing step.

The mechanism for the formation of ultra-thin films is outlined in Figure 12.

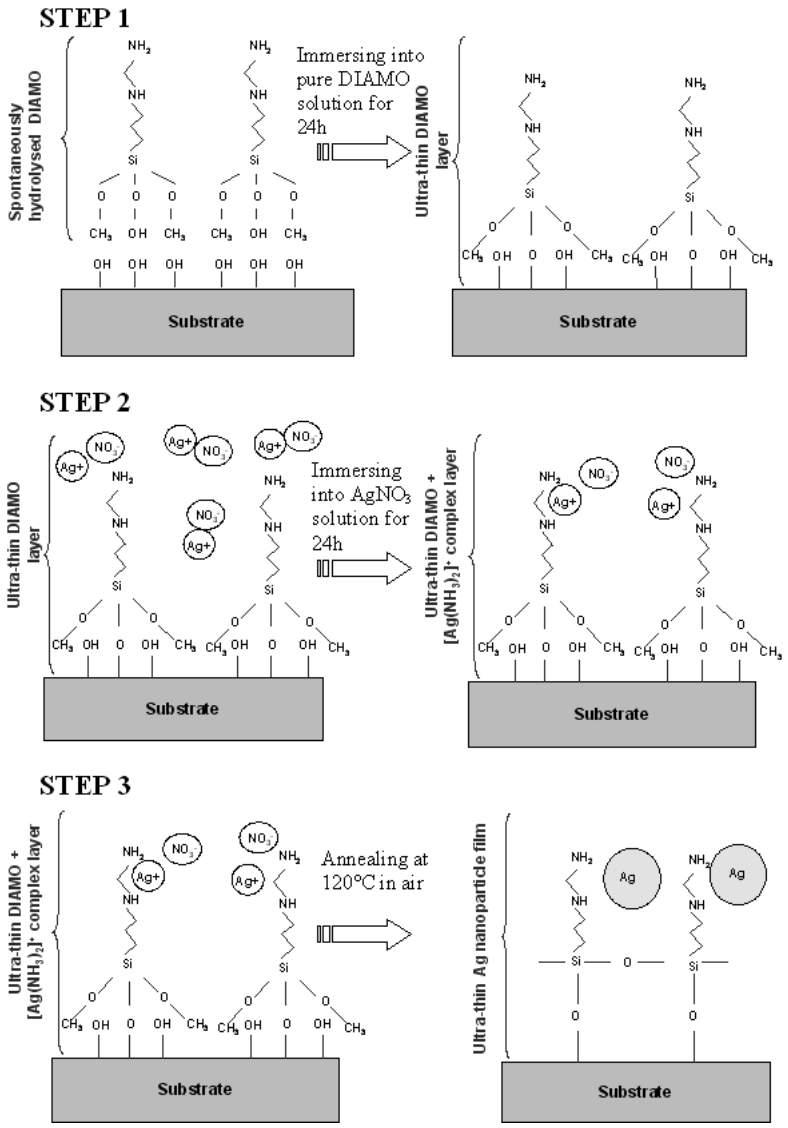

Figure 12. Schematic figure of the formation of ultra-thin films containing Ag nanoparticles using DIAMO as an anchoring molecule. Reproduced by permission of The Royal Society of Chemistry.

During Step 1, a small amount of spontaneously hydrolysed DIAMO is attached onto the surface by the trimethoxy silane head. When the sample is immersed into $AgNO_3$ solution for 24h (Step 2), $[Ag(NH_3)_2]$ complex is believed to form between the amino groups of attached DIAMO and silver ions, similar to the formation of the complex in ammonia solution[105]. The formation of silver nanoparticles takes place during the annealing step (Step 3). It is believed to occur simultaneously with the polymerisation

of silane groups of DIAMO which occurs during annealing just like in a normal silanisation process[106].

This reaction path resembles the formation Ag nanoparticle sols from a dissolved silver complex by reducing with different saccharides similar to the so called Tollens process or silver mirror test[6, 107] or the ones used in dry (photo)thermographic processes in which silver ions are reduced on the surface of a photographic plate during annealing in the presence of binders, stabilisers and reducers [108, 109]. The tight attachment of the Ag nanoparticles is achieved by utilising DIAMO: the silane head is assumed to react with the substrate surface whilst the other head is believed to attach the nanoparticle. The detailed nature of the binding is not the subject of this study but the aforementioned hypothesis is logical as DIAMO has been used successfully both as a binder between gold nanoparticles and silica particle surfaces[110] and a stabiliser for gold nanoparticles[111] or for silver nanoparticles in sol-gel matrices[84].

The characteristic values for the ultra-thin films were achieved through the analysis of AFM (measured by co-author) and FE-AES data. The average thickness of films prepared by this method was 4.7 nm and the silver coverage on the surface can be up to 5%. Furthermore, the height of Ag nanoparticles is approximately 9 nm and the width around 35 nm.

Further proof of the attachment of Ag nanoparticles is demonstrated by a simple dissolution test: the dissolution of silver into MQ water from Ag^+ ion containing samples (after Step 2, prior to annealing) is significantly higher (1.5 mg/l) than the dissolution of silver from nanoparticle containing films (after Step 3, annealed 120°C, 2h) which is only 0.4 mg/l.

3.5.2 SERS and Antibacterial Activity

Both the SERS and antibacterial activity of the samples were studied in collaboration with co-authors. Figure 13 shows the Raman spectra of a 10^{-4} M PMT

(phenylmercaptotetrazole) solution with (a) a known SERS probe (prepared in-house at Vrije Universiteit Brussels[112]), (b) a thicker film containing Ag nanoparticles - prepared by the same method as for the ultra-thin films but using *pre-hydrolysed* DIAMO - and (c) ultra-thin film containing silver nanoparticles (after Step 3, annealed for 2 h at 120°C).

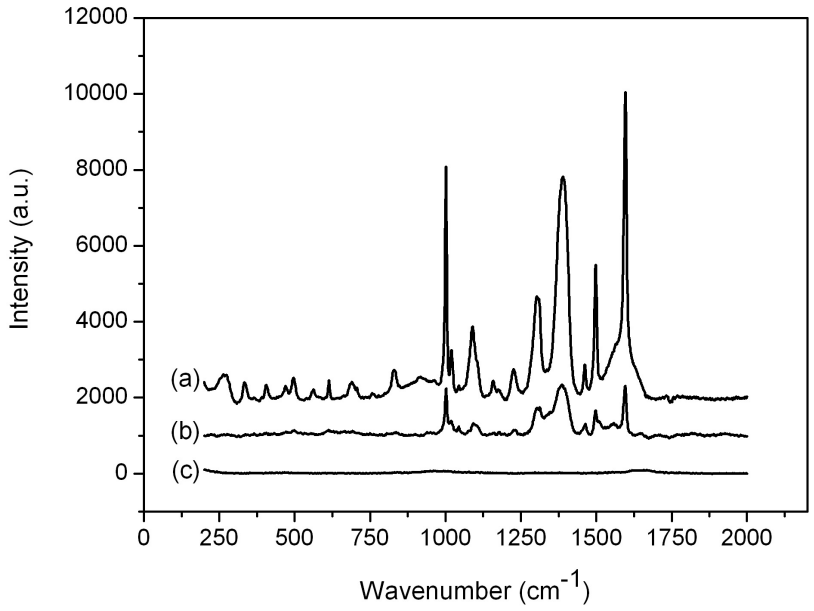

Figure 13. Raman spectra of PMT solution with a) a known SERS probe, b) a thicker film prepared exactly the same as ultra-thin films but using pre-hydrolysed DIAMO and c) an ultra-thin film. Reproduced by permission of The Royal Society of Chemistry.

When the spectra is measured with a SERS a probe a typical spectra for PMT is observed. In contrast, for the ultra-thin film no enhancement is detected. However, when the amount of Ag and DIAMO is increased through a creation of a thicker film SERS activity is observed. The main reason for the distinct difference in reactivity between the thicker and ultra-thin films is believed to be due to higher amount of Ag nanoparticles on the surface. The clearly yellow colour of thicker films can be easily seen even with the naked eye (unlike the ultra-thin films). As mentioned previously, typically a tiny amount of the molecules become adsorbed on the hot spots [69, 93],

therefore the enhancement is detectable only when a significant level of Ag nanoparticles are present to create SERS active areas.

The SERS enhancement factor (EF) can be calculated using Equation (9):

$$\mathrm{EF} = \frac{I(\text{surf of one molecule})}{I(\text{bulk of one molecule})} \tag{9}$$

where I(surf of one molecule) is the intensity which one PMT molecule on the studied surface contributes to the Raman spectra and I(bulk of one molecule) is the intensity which one PMT molecule of the pure substance contributes to Raman spectra.

PMT is the Raman active molecule and powder as a pure substance. Therefore, I(bulk) has been measured from the powder. However, the Raman intensity of PMT on the studied surface has been measured using a drop of 10^{-4} M solution of PMT. Therefore, a calculation of the number of molecules (which contribute to the total Raman intensity in question) has to be carried out in a different way for a solution and for a powder.

For a pure PMT powder, the amount of molecules contributing to the measured total intensity in a Raman spectrum can be estimated from the following equation:

$$\text{number of molecules} = \frac{A(\mathrm{L}) \cdot R}{A_{\mathrm{m}}} \tag{10}$$

where A(L) is area of laser hitting the surface (= powder), R is the roughness of the surface (= powder) and A_{m} is area of one PMT molecule.

For a PMT solution, the number of molecules can be calculated by estimating the volume through which the laser travels and number of particles in that volume:

$$\text{number of molecules} = c \cdot N_{\mathrm{A}} \cdot V(\mathrm{L}) \tag{11}$$

where c is the concentration of solution, N_{A} is Avogadro's number and V(L) is the volume of the laser (travelling through the solution to surface).

EF can be calculated by combining Equations 9-11 in the following:

$$\mathrm{EF} = \frac{I(\mathrm{surf})/\text{number of molecules}}{I(\mathrm{bulk})/\text{number of molecules}} = \frac{I(\mathrm{surf})/(c \cdot N_{\mathrm{A}} \cdot V(\mathrm{L}))}{I(\mathrm{bulk})/((A(\mathrm{L}) \cdot R)/A_{\mathrm{m}})} \quad (12)$$

where I(surf) is the total intensity of PMT molecules on the studied surface and I(bulk) is the total intensity of PMT powder.

The calculated estimations for the minimum values are: (i) for the probe EF is $8 \cdot 10^7$ and (ii) for the thicker film it is $1 \cdot 10^7$ (the ultra-thin film having no detectable enhancement).

Higher roughness value leads to higher EF value as can be seen from Equation 12. In the calculation of EF, the roughness value (R) for a powder has been selected to be 1 and in this way the result provides the lowest approximation for the enhancement factor. In reality, the factor is higher but a reliable estimation of the R value is somewhat difficult.

The antibacterial tests were performed using a clean glass slide as a reference sample and two different kinds of samples: 1) a sample containing Ag^+ ions (ultra-thin films before Step3, prior to annealing) and 2) the sample containing Ag nanoparticles (ultra-thin films after Step 3, annealing at 120°C for 2h). In addition, two different types of bacteria were tested, *E. coli* and *M. luteus*.

During the whole immersion time (24h) no detectable antibacterial activity towards *M. luteus* was observed with any of the samples. With *E. coli* the statistically significant inhibition for the sample that contains Ag^+ ions (sample before Step 3, prior to annealing) was detected only after 5 hours although, after 24h the inhibitive effect had disappeared. However, in the case of Ag nanoparticle containing samples no significant inhibition effect was observed.

This is in contrast to findings from earlier studies which suggest that Ag nanoparticle containing films are antibacterial. Although, in many of these studies, there is no discussion if the antibacterial behaviour is due to Ag^+ ions from dissolution of Ag nanoparticles rather than the nanoparticle itself [56,57] or from the unwelcome diffusion of

Ag nanoparticles out of the films into the surrounding environment before the dissolution step[61].

The results introduced in this Thesis indicate that Ag nanoparticles that are attached on the surface actually have no antibacterial nature in the measured test systems but an extra step which includes either the dissolution of Ag nanoparticles and/or Ag^+ ions is needed. However, it is worth noting that the ultra-thin films might still act as an antibacterial agent against bacteria which are not in a growing state and thus, also the development of new kind of test systems taking this into account is important.

3.6 Summary of Studies of Surface Modifications with Ag Nanoparticles

Two methods for surface modification with Ag nanoparticles have been outlined: the first one comprises of a more traditional sol-gel film in which Ag nanoparticles are embedded in silica matrix, and the latter one introduces a new method for the formation of ultra-thin films in which Ag nanoparticles are tightly attached on the surface.

The stability of TEOS based sol-gel films with Ag nanoparticles have been widely discussed in literature. This Thesis shows that stability can be improved by using low-temperature plasma treatments. Furthermore, in this study the effect of the nanoparticles and matrix has been studied. UV/Vis spectra show that changes in maximum absorbance can be related to the oxidation/reduction of the nanoparticles during the plasma treatments. The change in the centre of the peak, on the other hand, is primarily related to the matrix itself and to an excess of Ag^+ ion still present within it.

Due to the unknown health risks of metal nanoparticles there is also a clear need for the formation of films in which nanoparticles are tightly attached and their diffusion to the environment is inhibited. However, it is also important to test if these tightly attached

nanoparticles can still posses their superior properties such as SERS activity and antibacteriality.

A simple method to create ultra-thin films including three steps, 1) immersing the samples into DIAMO, 2) immersing samples into $AgNO_3$ solution and 3) annealing, has been developed. This procedure creates films which are almost imperceptible to the naked eye and in which nanoparticles are attached via DIAMO molecule both to glass and stainless steel surfaces. The nanoparticles are formed during the annealing step, most probably simultaneously with the polymerisation of DIAMO molecules.

When pre-hydrolysed DIAMO was used to create thicker films, the SERS activity is observed whilst with ultra-thin films detection is not possible. Most surprisingly, however, no antibacterial effect was observed with tightly bound nanoparticles even though some inhibition was detected with the films containing mainly Ag^+ ions. This indicates that tightly attached nanoparticles themselves do not possess antibacterial activity.

4 Conclusions

Two different kinds of approaches for surface modifications have been studied in this Thesis.

The first part of Thesis covers SECM studies of the formation of inhibitive [Cu(I)-BTA] film on different copper alloys. The use of SECM for the first time in such a system has produced answers for an old problem. The potential of copper has been found to be an important factor in the formation of an insulating film. Adsorption of BTAH molecule, that according to literature is believed to take place at negative potentials (lower than -0.3- (-0.2) V vs. SCE), does not create an insulating film on the copper surface. Instead, formation of the film is required and this takes place at more positive potentials. Furthermore, estimations of film thickness can be made and even though several rough assumptions must be used the values are in good agreement with literature.

Further studies of the inhibitive film show also that the presence of an alloying element can have a profound effect on the formation of the film, a result that has not been previously observed. During the electropolishing step silver most probably segregates on the surface which prevents the formation of the inhibitive [Cu(I)-BTA] film. In contrast, the other common alloying element, phosphorus, does not have such a strong influence on the film formation.

The role of oxygen in the formation of [Cu(I)-BTA] film has been under discussion for decades. This Thesis clearly demonstrates that oxygen is needed for the formation of the insulating film. The results also indicate that the molecular oxygen instead of Cu_2O can establish the formation. However, whether O_2 in solution first reacts with copper and only then Cu_2O is used in the film formation or O_2 alone can directly contribute to the film cannot be proved conclusively.

The second part of Thesis consists of the surface modifications with Ag nanoparticles. Firstly, the traditional sol-gel films with embedded Ag nanoparticles are studied. Using low-temperature O_2 and H_2 plasma treatments the stability and barrier properties of the studied sol-gel films can be improved. Especially interesting is the finding that the presence of Ag nanoparticles actually increases the barrier properties of the film in borate buffer solution, increasing the film resistance when compared to the sol-gel film without any nanoparticles.

Finally, a new approach for creating ultra-thin films which contain silver nanoparticles has been introduced and the mechanism for the formation has been suggested. First, the silver ions react with the DIAMO functionalised surface creating silver amino complexes and these complexes are further reduced to silver nanoparticles together with the polymerisation of DIAMO molecule.

Both the SERS and antibacterial properties of the film with tightly bound silver nanoparticles have been studied. SERS enhancement factor of a thicker film (prepared using pre-hydrolysed DIAMO) is more than $1 \cdot 10^7$. The antibacterial properties, however, could not be observed and this is believed to be due to a number of reasons: either the nanoparticles are tightly bound to the surface and their possible antibacterial nature is lost, or the antibacterial tests in which the bacteria is in a growing state is not the best method for testing such tightly bound silver nanoparticles.

In conclusion, this Thesis outlines two approaches for the surface modifications which are also of industrial significance; BTAH being a common inhibitor in copper industry and silver nanoparticles possessing several interesting properties such as SERS and antibacterial activity. The studies presented here clarify the understanding of [Cu(I)-BTA] film formation and the effects of potential, alloying element and oxygen on it. This Thesis also adds to the discussion of the actual role of Ag nanoparticles versus Ag^+ ions as antibacterial agents as well as of appropriate testing methods.

5 References

[1] W. Qafsaoui, Ch. Blanc, N. Pébère, A. Srhiri, G. Mankowski, *J. Appl. Electrochem.* **30** (2000) 959-966.

[2] M. Metikoš-Huković, R. Babić, I. Paić, *J. Appl. Electrochem*. **30** (2000) 617-624.

[3] P. Yu, D.-M. Liao, Y.-B. Luo, Z.-G. Chen, *Corrosion* **59** (2003) 314-318.

[4] J.-L. Yao, Y.-X. Yuan, R.-A. Gu, *J. Electroanal. Chem.* **273** (2004) 255-261.

[5] C.B. Murray, C. R. Kagan, M.G. Bawendi, *Annu. Rev. Mater. Sci*. **30** (2000) 545-610.

[6] A. Panáček, L. Kvítek, R. Prucek, M. Kolář, R. Večeřová, *J. Phys. Chem. B* **110** (2006) 16248-16253.

[7] K.A. Willets, R.P. Van Duyne, *Annu. Rev. Phys. Chem.* **58** (2007) 267-297.

[8] R.A. Caruso, M. Antonietti, *Chem. Mater.* **13** (2001) 3272-3282.

[9] P.H.M. Hoet, I. Brüske-Hochfeld, O.V. Salata, *J. Nanobiotechnology* **2 (**2004) 1-1-15.

[10] M.N. Moore, *Environment International* **32** (2006) 967-976.

[11] Stupnišek-Lisa, E., Cinotti, V., *J. Appl. Electrochemistry* **29** (1999) 117-122.

[12] E.M.M. Sutter, F. Ammeloot, M.J. Pouet, C. Fiaud, R. Couffignal, *Corr. Sci*. **41** (1999) 105-115.

[13] P. Yu, D.-M. Liao, Y.-B. Luo, Z.-G. Chen, *Corrosion* **59** (2003) 314-318 .

[14] D. Tromans, *J. Electrochem. Soc*. **145** (1998) L42-L45.

[15] V. Brusic, M.A. Frisch, B.N. Eldridge, B.N., F.B. Novak, F.B. Kaufman, B.M. Rush, G.S. Frankel, *J. Electrochem. Soc*. **138** (1991) 2253-2259.

[16] K. Cho, J. Kishimoto, T. Hashizume, H.W. Pickering, T. Sakurai, *Appl. Surf. Sci*. **87/88** (1995) 380-385.

[17] B.-S. Fang, C.G. Olson, D.W. Lynch, *Surf. Sci*. **176** (1986) 476-490 .

[18] J.-O. Nilsson, C. Törnkvist, B. Liedberg, *Appl. Surf. Sci.* **37** (1989) 306-326.

[19] O. Hollander, R. May, *Corrosion* **41** (1985) 39-44.

[20] J.F. Walsh, H.S. Dhariwal. A. Gutiérrez-Sosa, P. Finetti, C.A. Muryn, N.B. Brookes, R.J. Oldman, G. Thornton, *Surf. Sci.* **415** (1998) 423-432.

[21] R. Youda, H. Nishihara, K. Aramaki, *Electrochim. Acta* **35** (1990) 1011-1017.

[22] H. Y. Chan, M. J. Weaver, *Langmuir* **15** (1999) 3348-3355.

[23] C.H. Brooks, *Heat Treatment, Structure and Properties of Nonferrous Alloys*, American Society for Metals, USA, 1982, pp. 275- 285.

[24] J.R. Davis, P. Allen, *Metals Handbook Vol 2*, 10th ed., AMS International, 1990, pp. 265-267.

[25] P.G. Cao, J.L Yao, J.W. Zheng, R.-A. Gu, Z.Q Tian, *Langmuir,* **18** (2002) 100-104.

[26] Y. Ling, Y. Guan, K.N. Han, *Corrosion* **51** (1991) 367-375.

[27] Y. Jiang, J.B Adams, *Surf. Sci.* **529** (2003) 428-442.

[28] Z.D. Schultz, M. E. Biggin, J. O White, A. A. Gewirth, *Anal. Chem.* **76** (2004) 604-609.

[29] D. M. Bastidas, *Surf. Interface Anal.* **38** (2006) 1146-1152.

[30] E. Cano, J. L Polo, A. La Iglesia, J. M. Bastidas, *Adsorption* **10** (2004) 219-225.

[31] D. Tromans, R.-H. Sun, *J. Electrochem. Soc*. **138** (1991) 3235-3244.

[32] G. Xue, J. Ding, P. Lu, J. Dong, *J. Phys. Chem* **95** (1991) 7380-7384.

[33] A.J. Bard, *Introduction and Principles*, In book Scanning Electrochemical Micrscopy, Edited by A. J. Bard, M. Mirkin, Marcel Dekker, Inc USA, 2001, pp. 1-16.

[34] A. J. Bard, L.F. Faulkner, *Electrochemical Methods Fundamentals and Applications*, 2nd edition, John Wiley&Sons, Inc, USA, 2001, pp.168-176.

[35] I. Serebrennikova, H.S. White, *Electrochem. Solid-State Lett.* **4** (2001) B4-B6.

[36] I. Srebrennikova, S. Lee, H.S. White, *Faraday Discuss.* **12** (2002) 199-210.

[37] S. B. Basame, H.S. White, *J. Phys. Chem. B* **102** (1998) 9812-9819.

[38] S. B. Basame, H. S. White, *Anal. Chem.* **71** (1999) 3166-3170.

[39] K. Fushimi, K.A. Lill, H. Habazaki, *Electrochim. Acta* **52** (2007) 4246-4253.

[40] A. J. Bard, F.-R. F.Fan, M.V. Mirkin, *Scannign Electrochemical Micrsocopy*, In book: Electroanalytical Chemistry, ed. by A. J. Bard, Marcel Dekker, USA, 1994, pp.243-373.

[41]M. V. Mirkin, *Theory*, In book: Scanning Electrochemical Microscopy, ed.by A. J. Bard, M. Mirkin, Marcel Dekker, Inc, USA, 2001, pp. 145-199.

[42] K. Brogwarth, J. Heinze, *Heterogeneous Electron Transfer Reactions*, In book: Scanning Electrochemical Micrscopy, Edited by A. J. Bard, M. Mirkin, Marcel Dekker, Inc USA, 2001, pp. 201-240.

[43] Babić, R, Metikoš-Huković, M., Lončar, M., *Electrochim. Acta* **44** (1999) 2413-2421.

[44] A. Frignani, M. Fonsati, C. Monticelli, G. Brunoro, *Corros. Sci.* **41** (1999) 1217-1227.

[45] M. Bojinov, G. Fabricius, P. Kinnunen, T. Laitinen, K. Mäkela, T. Saario, G. Sundholm, *J. Electroanal. Chem.* **504** (2001) 29-44.

[46] B. Beverskog, M. Bojinov, P. Kinnunen, T. Laitinen, K. Mäkelä, T. Saario, *Corros. Sci.* **44** (2002) 1923-1940.

[47] W. Mehnert, K. Mäder, *Advanced Drug Delivery Reviews* **47** (2001) 165-196.

[48] W. J. Parak, L. Manna, F.C. Simmel, D. Gerion, P. Alivisatos, *Quantum Dots*. In book: Nanoparticles – From theory to Application, ed. by G. Schmid, Wiley-VHC Verlag GmbH& Co KGaA, Weinheim, Germany, 2004, pp. 4-49.

[49] B. V. Enüstün, J. Turkevich, *J. Am. Chem. Soc.* **85** (1963) 3317-3328.

[50] M. Brust, M. Walker, D. Bethell, D.J. Schiffrin, R. Whyman, *J.Chem. Soc., Chem. Commun.* **7** (1994) 801-802.

[51] A. Taleb, C. Petit, M.P. Pileni, *Chem. Mater.* **9** (1997) 950-959.

[52] V. Sambhy, M.M. MacBride, B.R. Peterson, A. Sen, *J. Am. Chem. Soc.* **128** (2006) 9798-9808.

[53]A.Vaškelis, A. Jagminienė, L. Tamašauskaitė-Tamašiūnaitė, R. Juškėnas, *Electrochim. Acta* **50** (2005) 4586-4591.

[54] B. S. Atiyeh, M. Cotagliola, S.H. Hayek, S. A. Dibo, *Burns* **33** (2007) 139-148.

[55] H.J. Klasen, *Burns* **26** (2000) 131-138.

[56] J. Dai, M. L. Bruening, *Nano Lett.* **2** (2002) 497-501.

[57] Z. Shi, K.G. Neoh, E.T. Kang, *Langmuir* **20** (2004) 6847-6852.

[58] N. Simonetti, G. Simonetti, F. Bougnoil, M. Scalzo, *Appl. Environ. Microbiol*. **58** (1992) 3834-3836.

[59] J. C. Grunlan, J. K. Choi, A. Lin, *Biomacromolecules* **6** (2005) 1149-1153.

[60] C.-N. Lok, C.-M. Ho, R. Cheng, Q-Y. He, W.-Y. Yu, H. Sun, P. K.-H. Tam, J.-F. chiu, C.-M. Che, *Journal of Proteome Research* **5** (2006) 916-924.

[61] D. Lee, R. E. Cohen, M. F. Rubner, *Langmuir* **21** (2005) 9651-9659.

[62] Z. Li, D. Lee, X. Sheng, R.E. Cohen, M. F. Rubner, *Langmuir* **22** (2006) 9820-9823.

[63] Q. Wang, H. Yu, L. Zhong, J. Liu, J. Sun, J. Shen, *Chem. Mater.* **18** (2006) 1988-1994.

[64] P.W. Atkins, Physical Chemistry, Oxford University Press (1998), pp. 457, 472-475, 488-491, 853.

[65] J. O'M Bockris, S. U. M. Khan, *Surface Electrochemistry A Molecular Level Approach*, Plenum Press, New York, 1993, pp. 43.

[66] M. Fleischmann, P.J. Hendra, A.L. McQuillan, *Chem. Phys. Lett.* **26** (1974) 163-166. In Ref: J. O'M Bockris, S. U. M. Khan, Surface Electrochemistry A Molecular Level Approach, Plenum Press, New York, 1993, pp. 43.

[67] M. L. Jacobson, K. L. Rowlen, *J. Phys. Chem. B* **110** (2006) 19491-19496.

[68] A. Campion, P. Kambhampati, *Chem. Soc. Rev.* **27** (1998) 241-250.

[69] S. Nie, S. R. Emory, *Science* **275** (1997) 1102-1107.

[70] R. F. Aroca, P. J. G. Goulet, D. S dos Santos, R. A. Alvarez-Puebla, O.N. Oliveira, *Anal. Chem.* **77** (2005) 378-382 .

[71] Y. Wang, X. Zou, W. Ren, W. Wang, E. Wang, *J. Phys. Chem. C* **111** (2007) 3259-3265.

[72] P. Chakraborty, *J. Mater. Sci.* **33** (1998) 2235-2249.

[73] P.D. Townsend, D.E. Hole, *Vacuum* **63** (2001) 641-647.

[74] N. Bloembergen, *IEEE J. Sel. Top. Quantum Electron.* **6** (2000) 876-880.

[75] J.J. Ebelmen, *Ann.* **57** (1846) 331. In Refs: C.J. Brinker, G.W. Scherer, Sol-Gel Science – The Physics and Chemistry of Sol-Gel Processing , Academic Press, USA, 1990, pp. 1-18; H. Distlich, Thin Films from the Sol-Gel Process, In Book: Sol-Gel Technology for Thin Films, Fibers, Preforms, Electronic and Specialty Shapes, ed. by L.C. Klein, Noyes Publications, USA, 1988, pp.50-78.

[76] W. Geffken and E. Berger, German Patent 736 411 (May 1939). In Refs: C.J. Brinker, G.W. Scherer, Sol-Gel Science – The Physics and Chemistry of Sol-Gel Processing , Academic Press, USA, 1990, pp. 1-18; H. Distlich, Thin Films from the Sol-Gel Process, In Book: Sol-Gel Technology for Thin Films, Fibers, Preforms, Electronic and Specialty Shapes, ed. by L.C. Klein, Noyes Publications, USA, 1988, pp.50-78.

[77] C.J. Brinker, G.W. Scherer, *Sol-Gel Science – The Physics and Chemistry of Sol-Gel Processing* , Academic Press, USA, 1990, pp. 1-18, 97-233.

[78] H. Distlich, *Thin Films from the Sol-Gel Process*, In Book: Sol-Gel Technology for Thin Films, Fibers, Preforms, Electronic and Specialty Shapes, ed. by L.C. Klein, Noyes Publications, USA, 1988, pp.50-78.

[79] Y.-S. Li, P.B. Wright, R. Puritt, T. Tran, *Spectrochim. Acta, Part A* **60** (2004) 2759-2766.

[80] L. Armelao, R. Bertoncello, E. Cattaruzza, S. Gialanella, S. Gross, G. Mattei, P. Mazzoldi, E. Tondello, *J. Mater. Chem.* **12** (2002) 2401-2407.

[81] F.H. Scholes, S.A. Furman, D. Lau, C.R. Rossouw, T.J. Davis, *J Non-Cryst. Solids* **347** (2004) 93-99.

[82] H.-J. Jeon, S.-C. Yi, S.-G. Oh, *Biomaterials* **24** (2003) 4921-4928.

[83] G. De, A. Licciucilli, C. Massaro, L. Tapfer, M. Catalano, G. Battaglin, C. Meneghini, P. Mazzoldi, *J. Non-Cryst. Solids* **194** (1996) 225-234.

[84] M. Mennig, M. Schmitt, H. Schmidt, *J. Sol-Gel Sci. Technol.* **8** (1997) 1035-1042.

[85] H. Bi, W. Cai, L. Zhang, D. Martin, F. Träger, *Appl. Phys. Lett.* **81** (2002) 5222-5224.

[86] G. De, D. Kundu *J. Non-Cryst. Solids* **228** (2001) 221-225.

[87] V. Hornebecq, M. Antonietti, T. Cardinal, M. Treguer-Delapierre, *Chem. Mater.* **15** (2003) 1993-1999.

[88] A.L. Pan, H.G. Zheng, Z.P. Yang, F.X. Liu, Z.J. Ding, Y.T. Qian, *Mater. Res. Bull.* **38** (2003) 789-796.

[89] A. Babapour, O.Akhavan, R. Azimirad, A. Z. Moshfegh, *Nanotechnology* **17** (2006) 763-771.

[90] B. Ritzer, M.A. Villegas, J.M. Fernández Navarro, *J. Sol-Gel Sci. Technol.* **8** (1997) 917-921.

[91] S. Shibata, K. Miyajima, Y. Kimura, T. Yano, *J. Sol-Gel Sci. Technol.* **31** (2004) 123-130.

[92] K. Sarkar, F. Cloutier, M.A. El Khakani, *J. Appl. Phys.* **97** (2005) 084302-1 - 084302-5.

[93] K. Kneipp, Y. Wang, R.R. Dasari, M.S. Feld, *Appl. Spectrosc.* **49** (1995) 780-784.

[94] L. Netzer, J. Savig, *J. Am. Chem. Soc.* **105** (1983) 674-676.

[95] H. Lee, L.J. Kepley, H.-G. Hong, T. E. Mallouk, *J. Am. Chem. Soc.* **110** (1988) 618-620.

[96] H. C. Yang, K. Aoki, H.-G. Hong, D.D. Sackett, M.F. Arendt, S.-L. Yau, C.M. Bell, T.E. Mallouk, *J. Am. Chem. Soc.* **115** (1993) 11855-11862.

[97] A. Babtiste, A. Gibaud, J.F. Bardeau, K. Wen, R. Maoz, J. Savig, B.M. Ocko, *Langmuir* **18** (2002) 3916-3922.

[98] C. Lu, S. Bai, D. Zhang, L. Huang, J. Ma, C. Luo, W. Cao, *Nanotechnology* **14** (2003) 680-683.

[99] M. D. Musick, C. D. Keating, L. A. Lyon, S. L. Botsko, D. J. Peña, W. D. Holliway, T. M. McEvoy, J. N. Richardson, M. J. Natan, *Chem. Mater.* **12** (2000) 2869-2881.

[100] K. Esumi, S. Akiyama, T. Yoshimura, *Langmuir* **19** (2003) 7679-7681 .

[101] D.-J. Qian, C. Nakamura, T. Ishida, S.-O. Wenk, T. Wakayama, S. Takeda, J. Miyake, *Langmuir* **18** (2002) 10237-10242 .

[102] J. Liu, L. Cheng, Y. Song, B. Liu, S. Dong, *Langmuir* **17** (2001) 6747-6750 .

[103] L. Supriya, R. O. Claus, *J. Phys.Chem. B* **109** (2005) 3715-3718 .

[104] M. Riskin, B. Basnar, V. I. Chegel, E. Katz, I. Willner, F. Shi, X. Zhang, *J. Am. Chem. Soc.* **128** (2006) 1253-1260.

[105] Y. Saito, J.J. Wang, D.N. Batchelder, D.A Smith, *Langmuir* **19** (2003) 6857-6861.

[106] C.M. Halliwell, A.E.G. Cass, *Anal. Chem.* **73** (2001) 2476-2483.

[107] L. Kvitek, R. Prucek, A. Panáček, R. Novotný, J. Hrbác, R. Zbořil, R. *J. Mater. Chem.* **15** (2005) 1099-1105.

[108] E. Tourwé, "Towards a quantitative description of electrochemical reactions: a spectro-electrochemical study of the reduction of silver ions" PhD Thesis, Vrije Universiteit Brussel, Brussels, 2005; pp. 3-13.

[109] A.S Diamond, D.S Weiss, *Handbook of Imaging Materials*, 2nd Ed., Marcel Dekker, New York, 2002, pp. 473-529.

[110] S.L. Westcott, S.J. Oldenburg, T.R. Lee, N.J. Halas, *Langmuir* **14** (1998) 5396-5401.

[111] B. Kutsch, O. Lyon, M. Schmitt, M. Menning, O. Schmidt, *J. Non-Cryst. Solids*, **217** (1997) 143-154 .

[112] R.D. Mondt, K. Baert, I. Geuens, L. van Vaeck, A. Hubin, *Langmuir,* **22** (2006) 11360-11368.

ISBN 978-951-22-9226-4
ISBN 978-951-22-9227-1 (PDF)
ISSN 1795-2239
ISSN 1795-4584 (PDF)